Phase Separation and Gelation in Solutions and Blends of Hetero-Associative Polymers

Scott P. O. Danielsen,*,† Alexander N. Semenov,‡ and Michael Rubinstein*,†,¶,§

†*NSF Center for the Chemistry of Molecularly Optimized Networks, Soft Matter Center, and Thomas Lord Department of Mechanical Engineering and Materials Science, Duke University, Durham, NC 27708, United States*

‡*Institut Charles Sadron, Centre National de la Recherche Scientifique UPR 22, Université de Strasbourg, 23 rue du Loess, BP 84047, 67034 Strasbourg Cedex 2, France*

¶*Departments of Physics, Chemistry, and Biomedical Engineering, Duke University, Durham, NC 27708, United States*

§*World Primer Institute for Chemical Reaction Design and Discovery (WPI-ICReDD), Hokkaido University, Kita 21 Nishi 10, Kita-ku, Sapporo, Hokkaido, 001-0021, Japan*

E-mail: scott.danielsen@duke.edu; michael.rubinstein@duke.edu

For Table of Contents use only
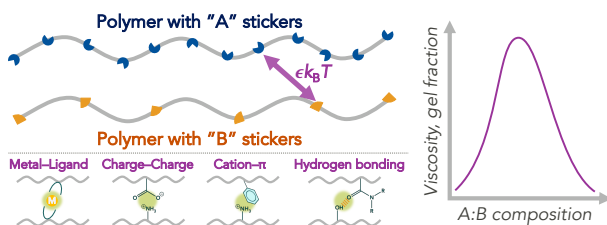
Abstract

An equilibrium statistical mechanical theory for the formation of reversible networks in two-component solutions of associative polymers is presented to account for the phase behavior due to hydrogen bonding, metal–ligand, electrostatic, or other pairwise heterotypic associative interactions. We derive explicit analytical expressions for the binding statistics, gelation condition, and free energy, in which we consider polymers of types A and B with many associating groups per chain and consider only $A - B$ association between the groups. The free energy is approximated at the mean-field level, considering overlapping polymer chains with an ideal gas of "stickers" capable of intermolecular association. It is shown that the number of associations is maximized at stoichiometric conditions between A and B associative groups. Accordingly, homogeneous networks are most easily formed near stoichiometric conditions between A and B associative groups, resulting in a re-entrant sol–gel–sol transition as the overall composition is altered. Association and reversible network formation are found to be accompanied by a tendency for phase separation. These results demonstrate that reversibly associating polymers have a large parameter space in terms of molecular design, binding energy, and mixture compositions. Our predictions are expected to be useful in the rational design of interacting polymer mixtures and the formation of reversible networks.

1 Introduction

Polymer networks are complex systems of components connected by physical and chemical associations, presenting an opportunity to exert molecular-level control of the network connectivity and macroscopic material properties.[1–3] In particular, polymers linked by reversible associations are an evolving class of materials exhibiting promising properties attributed to their dynamic nature. The transient cross-linking enables self-healing or remendability, with the materials able to re-develop their structure and properties after failure or re-processing.[4–8] The dynamic bonding further enables stimuli-responsiveness, permitting modulation of the composition, morphology, and viscoelastic properties through control of the associations by temperature, pH, salt, mechanical force, etc.[8,9] Such responsive, transient associations form the basis of many synthetic and biological systems, such as rheological modifiers, thermoplastic elastomers, chromatin transcription, and subcellular compartmentalization.[1,10–20]

The reversible cross-links between different chains are a result of specific associations between associating groups, also denoted as "stickers". These stickers can exist as free, open to potential association, or closed, already associated with another sticker. The associations can be saturable, in that only a specified number of stickers can participate, typically two, or be non-saturable, with many stickers associating per aggregate. While the latter can include block copolymers, which form micellar or other self-assembled structures, most associating polymers contain a low fraction of sticky sites distributed along the chain, separated by "spacers" of non-associating monomers. Multifunctional associative polymers, with multiple stickers per chain, result in the formation of supramolecular structures ranging from loopy single-chain nanoparticles to network gels.[21–26]

Most reversible cross-links are formed by attractive short-ranged physical interactions. A variety of different supramolecular (or non-covalent) interactions exist in nature and have been explored for the development of novel materials. Importantly, these associations can be *homotypic*, in which one type of sticker can self-associate both intra- and intermolecularly, or *heterotypic*, in which stickers of different types associate (Figure 1). Homo-associative

interactions include generalized hydrophobic interactions, occurring from weak van der Waals forces (and from effective repulsion between nonpolar groups and polar solvent molecules), $\pi - \pi$ stacking of aromatic moieties, and dipolar interactions. The best studied examples of networks formed from such $A - A$-type interactions are ionomers, polymers with a sparse number of charged monomers. In the melt state, the overall dielectric constant of the material is low, causing the charge-compensating counterions to condense and bind to the opposite charges on the chain, resulting in dipoles that then effectively cross-link the material by ionic clustering.[27–30] Notably, these systems motivated the development of the first reversible network theories for their static and dynamic properties,[6,31–40] expanding beyond the classical gelation models of Flory and Stockmayer.[41–44]
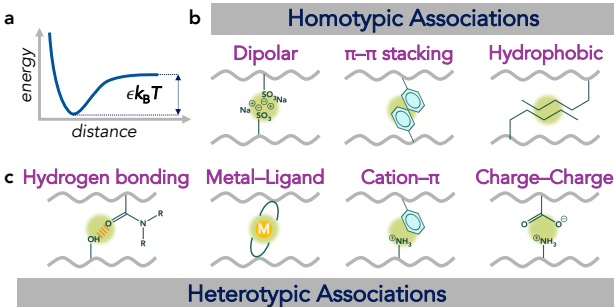

Figure 1: Schematic illustration of (a) free energy profile of reversible association of depth $\epsilon k_{\mathrm{B}}T$, (b) homotypic $(A - A)$ interactions, such as dipolar, $\pi - \pi$, and hydrophobic, and (c) heterotypic $(A - B)$ interactions, such as hydrogen bonding, metal–ligand, cation–π, and charge–charge (ionic bonds).

However, in many systems, the stickers hetero-associate, forming $A - B$ linkages, either between different sections of a heteropolymer, or between different chains in a mixture of associating polymers. Examples of hetero-complementary associations include hydrogen bonding,[45,46] ionic bonds between charges of opposite sign,[47,48] metal–ligand coordination,[49–53] host–guest interactions,[54,55] cation–π stacking,[56] or Lewis acid–base pairs.[57] The diversity of heterotypic associations provides a wide range of association strengths (or affinities), which broadens the design space for new reversible networks.[58–60]

In general, these sticker associations are weaker than permanent covalent bonds; the

lifetime of their bonds is finite and on realizable time scales. However, the strength of associations and resulting bond lifetimes can vary by many orders of magnitude (Figure 2). Depending on the nature of the associative interactions relative to the thermal energy, $k_\mathrm{B}T$, the cross-links can be effectively irreversible, with pseudo-permanent bonds, or so short-lived that the system is nearly indistinguishable from a non-bonding solution or melt. Intermediate to those limits, the lifetime of the associations is observable, and cross-links readily break and re-form.
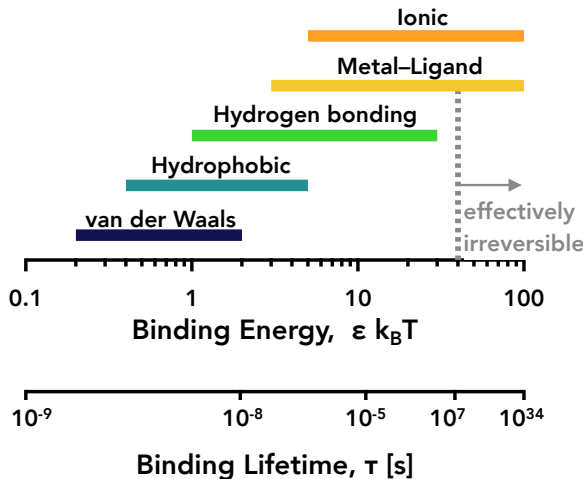

Figure 2: Typical binding strengths $\epsilon\, k_\mathrm{B}T$ and lifetimes τ of non-covalent associative interactions. Binding lifetimes are estimated by $\tau = \tau_0 \exp\left(\epsilon\right)$, where $\tau_0 \approx 10^{-9}$ s for caging in liquids. Interactions with binding energies above $\sim 40\, k_\mathrm{B}T$ correspond to binding lifetimes longer than 5 years and are considered effectively irreversible.

While the quantum chemical mechanisms of how each of these attractive interactions cause chain segments to stick and un-stick are vastly different, each can be considered as a "sticky" interaction imparting additional monomeric friction and connectivity constraints in the material. There exists a need to understand how the hetero-complementary character of such interactions affects the overall material properties. Painter and Coleman first recognized the unique interplay of entropy and enthalpy in hydrogen bonding,[61] arguing simple modifications to Flory–Huggins theory were inadequate.[62–64] Since then, various theories have been developed to describe different case studies of associating polymer mixtures, focusing on specific interaction regimes, polymeric structure, or other solution conditions.[65–76]

Recently, the complexation of oppositely charged polyelectrolytes, in particular, has been widely studied, providing a wealth of predictions for binary associative polymer solutions with long-range electrostatic interactions.[77–87]

Here, we extend an equilibrium statistical mechanical theory for the thermodynamics and gelation of associative polymers[32] to the case of heterotypic $A - B$ interactions. Transient binding between hetero-complementary associating groups compatibilizes the mixture, resulting in effective branched block copolymers and ultimately the formation of multi-component copolymer networks. Since homogeneous networks are most easily stabilized near stoichiometric conditions between A and B associative groups, altering the overall composition results in a re-entrant sol–gel–sol transition. It is shown that association and formation of a reversible network are always accompanied by a tendency for phase separation, albeit suppressed (to higher association strengths) in relation to self-associative polymers. We expect that this theoretical framework and resulting predictions will be useful for describing the behavior of polymers containing hydrogen bonding, metal–ligand, electrostatic, or other heterotypic pairwise associative interactions, as well as designing new molecularly optimized reversible networks.

2 Model

As a minimal model system, consider a solution of linear chains with associating groups (stickers) of type $i = A, B$ (Figure 3). Each chain of length N_i contains f_i stickers ($2 \ll f_i \ll N_i$), separated by spacers with $s_i = N_i/(f_i - 1)$ which is asymptotically $s_i \simeq N_i/f_i$ for $f_i \gg 1$ monomers. Since we consider sticky associations at the mean-field level without correlations, the specific distribution of stickers along the chain does not affect the thermodynamics. Stickers can associate in saturable $A - B$ pairs with the energy of association equal to $\epsilon \, k_{\mathrm{B}}T$, where $k_{\mathrm{B}}T$ is the thermal energy. Assuming monomers of type $i = A, B$ have the same size a, the monomer concentration of type i in solution is c_i, the number density of polymer

chains is c_i/N_i, and the number density of stickers is $f_i c_i / N_i \simeq c_i / s_i$. The number of stickers in volume V is

$$N_{\text{st},i} = f_i \frac{c_i}{N_i} V \simeq \frac{c_i}{s_i} V \qquad (2.1)$$

Let p_i be the fraction (probability) of stickers of type i that are associated in a bound $A - B$ pair (i.e., the degree of conversion of type i). The number of such pairs of associated stickers in volume V is,

$$N_{\text{p}} = p_i N_{\text{st},i} \qquad (2.2)$$

Thus, the number density of temporary bonds (pairs of stickers) is

$$\rho = \frac{N_{\text{p}}}{V} = p_i \frac{f_i c_i}{N_i} \simeq p_i \frac{c_i}{s_i} \qquad (2.3)$$

While we will stray away from this nomenclature, we should note that in the context of biological applications of such a sticker–spacer model, the number of stickers per molecule is commonly referred to as the "valency" or "multivalency".[88–90]
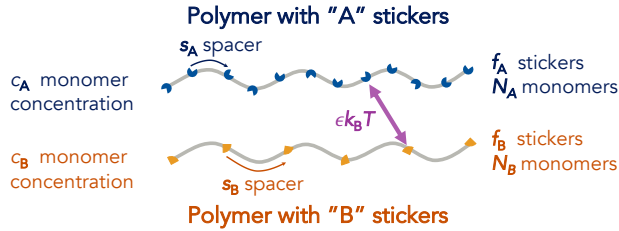

Figure 3: Model system of $A - B$ associative polymers.

The free energy density of this system can be written:

$$\frac{F}{k_{\text{B}}T} = \frac{c_A}{N_A} \ln\left(c_A a^3\right) + \frac{c_B}{N_B} \ln\left(c_B a^3\right) + \frac{v}{2}(c_A + c_B)^2 + \frac{w}{6}(c_A + c_B)^3 + \chi_{AB} a^3 c_A c_B$$
$$+ \rho + \frac{c_A}{s_A} \ln\left(1 - p_A\right) + \frac{c_B}{s_B} \ln\left(1 - p_B\right) \quad (2.4)$$

where v is the excluded volume parameter describing the solvent quality, w is the three-body interaction parameter, χ_{AB} is the Flory–Huggins interaction parameter between A

and B segments, and a^3 is the monomeric volume. The first two terms of eq. 2.4 are the ideal-gas translational entropy of the polymer chains, and the next three terms are the interaction energy from two- and three-body interactions and chemical contacts. Collectively, these terms are the traditional expression of the free energy for a non-associating mixture of polymers A and B in solution.[91–94] The last three terms in eq. 2.4 account for the association of stickers. The combinatorial entropy of the sticker bonds is expressed as $\rho\,k_{\mathrm{B}}T$, which is $k_{\mathrm{B}}T$ per bound sticker pair. The entropy of the unpaired A and B stickers is described by $(c_A/s_A)\ln(1-p_A)$ and $(c_B/s_B)\ln(1-p_B)$, respectively. The sticker association enthalpy (and its dependence on the binding strength $\epsilon\,k_{\mathrm{B}}T$) is incorporated implicitly through the degrees of conversion $(p_A,\,p_B)$, a consequence of the free energy minimization. Note that p_A and p_B are related to the number density of temporary bonds ρ, $p_A = \rho s_A/c_A$, $p_B = \rho s_B/c_B$, while ρ is related to ϵ by virtue of a mass action law (eqs. 3.14, A.13, A.14). For clarity and conciseness, the remaining details and derivation of the model thermodynamics are relegated to the Appendix.

The results presented in this work correspond to a mean-field theory, in which we have neglected correlations between sticker positions. Accordingly, the theory is not applicable in the dilute regime, rather we must demand that the coils are strongly overlapping, i.e., a semidilute or concentrated solution. More precisely, our mean-field approach is valid if there are typically many stickers in a sphere of radius $as_i^{1/2}$ equal to the size of a spacer s_i:

$$(c_i/s_i)(as^{1/2})^3 = c_i a^3 s_i^{1/2} \gg 1 \tag{2.5}$$

In other words, we assume that the spacers are overlapping.

The free energy of association depends on the concentration of A and B stickers c_i/s_i and their degrees of conversion only and does not explicitly depend on either the numbers of stickers per chain f_i, nor on the degrees of polymerization N_i. In mean-field, this free energy is approximated as that of a mixture of stickers. This approximation is valid when

concentration blobs are not swollen by excluded-volume monomer interactions, i.e., in the semidilute Θ and concentrated regimes:[95,96]

$$v/a^6 \ll c_A + c_B \tag{2.6}$$

where the conformational statistics of polymer chains are nearly Gaussian. Accordingly, we will initially set $v = 0$ and $w = a^6$ to describe Θ solutions: $va^3 \ll w/\sqrt{s_i}$. We will relax this constraint to arbitrary v to describe good and athermal solvents in a subsequent paper. Following de Gennes,[97] we further assert that the parameters v, w, and χ_{AB} are not directly affected by the presence of cross-links, which should be true for long overlapping strands between stickers, $s_i \gg 1$.

3   Bound Sticker Pair Formation

The fraction of paired stickers is the primary parameter governing the static and dynamic properties of associating polymers. The fractional degree of conversion can be obtained using eq. A.13,

$$p_A = \frac{p_B}{r} = \frac{1}{2}\left[1 + r^{-1} + \frac{1 - r^{-1}\sqrt{\left(r + (1+r)\frac{c_A}{s_A}\lambda\right)^2 - r\left(2\frac{c_A}{s_A}\lambda\right)^2}}{\frac{c_A}{s_A}\lambda}\right] \tag{3.1}$$

and is a function of two parameters: the attractive volume fraction of the stickers, $\lambda c_A/s_A$, and the stoichiometric ratio of the sticker concentrations,

$$r = \frac{c_A/s_A}{c_B/s_B} = \frac{p_B}{p_A}. \tag{3.2}$$

In eq. 3.1 we have defined an association strength,

$$\lambda \equiv v_{\mathrm{b}} \exp\left(\epsilon\right) \tag{3.3}$$

with the volume of a bond v_b and energy of association $\epsilon\, k_B T$. This can be described as the attractive volume of a bond, an effective capture volume around a sticker. Eq. 3.1 highlights the two manners for controlling the association behavior: either by increasing the sticker concentrations c_i/s_i and their association strength, λ, or by balancing the availability of their complementary stickers. While the degrees of conversion of A and B can be maximized by either approach, the total number density of reversible bonds $\rho = p_A c_A/s_A = p_B c_B/s_B$ is only maximized by increasing the product of the degrees of conversion and number densities of stickers.

3.1 Stoichiometric Mixtures

To understand the effects of pairwise hetero-association on the degree of conversion, it is then useful to compare the degree of conversion of sticker A,

$$p_A = \frac{1}{2}\left[1 + \frac{c_B/s_B}{c_A/s_A} + \frac{1 - \sqrt{\left(1 + \left(\frac{c_A}{s_A} + \frac{c_B}{s_B}\right)\lambda\right)^2 - 4\frac{c_A}{s_A}\frac{c_B}{s_B}\lambda^2}}{\frac{c_A}{s_A}\lambda}\right] \tag{3.4}$$

equivalent to eq. 3.1, with the homo-binding $(A - A)$ case:[32]

$$p_A = 1 + \frac{1 - \sqrt{4\frac{c_A}{s_A}\lambda + 1}}{2\frac{c_A}{s_A}\lambda} \quad \text{for } A - A \text{ homo-association} \tag{3.5}$$

For sticker-stoichiometric mixtures, with equal number densities of A and B stickers (i.e., $c_A/s_A = c_B/s_B$ and $r = 1$, eq. 3.2), the degree of conversion for the $A - B$ system is quantitatively identical to that for $A - A$ (Figure 4a); the probability of closed pairs of $A - B$ stickers is equal to that for closed pairs of $A - A$ stickers at the same concentrations of A stickers. Importantly, however, while $\lambda c_A/s_A$ and thus, p_A, are the same, in the $A - B$ case, there are twice as many stickers $(c_A/s_A + c_B/s_B)$ and therefore twice as many bonds (i.e., $\rho_{A-B} = 2\rho_{A-A}$). Accordingly, for equivalent total concentration of stickers, at the same

association strength, the need for A stickers to have B stickers for hetero-bonding limits the accessible number of bound sticker pairs and degree of conversion due to self-dilution.
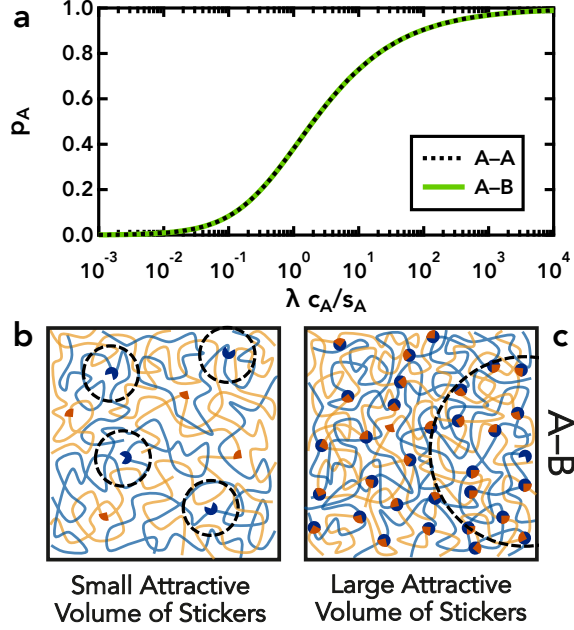

Figure 4: (a) Degree of conversion of A stickers, p_A, for a Θ-solution of associating polymers of type $A - A$ (with c_A/s_A) and $A - B$ (with $c_A/s_A = c_B/s_B$) as a function of increasing attractive volume fraction of stickers $\lambda c_A/s_A$. Schematic illustrations of $A - B$ system at (b) low and (c) high attractive volume fraction of stickers $\lambda c_A/s_A$. A stickers are denoted by blue major sectors and B stickers are denoted by orange minor sectors, as in Figure 3. Closed sticker pairs are indicated by the union of these blue and orange sectors. The attractive volumes of a bond (around unpaired A stickers) are marked by dashed circles.

Considering heterotypic associations in a mixture of A and B polymers under stoichiometric conditions ($r = 1$, or correspondingly $c_A/s_A = c_B/s_B$), the degree of conversion $p_A = p_B$ has two limiting behaviors. Below the overlap of attractive volumes of stickers, $\lambda c_A/s_A = \lambda c_B/s_B \ll 1$, the probability that stickers of A and B will find each other is low, and the degree of conversion is small (Figure 4b). For low fraction of bonds, the degree of conversion p_i increases linearly with and approximately equal to the attractive volume fraction of stickers ($\lambda c_i/s_i$):

$$p_A = p_B \simeq \lambda \frac{c_A}{s_A} \simeq \lambda \frac{c_B}{s_B} \quad \text{for} \quad \lambda \frac{c_A}{s_A} = \lambda \frac{c_B}{s_B} \ll 1 \tag{3.6}$$

This limit corresponds to non-overlapping attractive volumes of stickers, in which the degree of conversion of A, p_A, is the probability of an A sticker being within the attractive volume of a B sticker.

In the opposite limit, above the overlap of attractive volumes of stickers, $\lambda c_A/s_A = \lambda c_B/s_B \gg 1$, most stickers of A and B easily find complementary stickers with which to bond, as nearly all stickers are within the attractive volumes of potential sticker partners (Figure 4c). Accordingly, most stickers are bound,

$$p_A = p_B \simeq 1 - \sqrt{\frac{s_A}{\lambda c_A}} \simeq 1 - \sqrt{\frac{s_B}{\lambda c_B}} \quad \text{for} \quad \lambda \frac{c_A}{s_A} = \lambda \frac{c_B}{s_B} \gg 1 \tag{3.7}$$

and the fractional degrees of conversion approach unity, i.e., full conversion in which all stickers are paired.

3.2 Non-Stoichiometric Mixtures

Importantly, because a heterotypic reversible bond requires both an A sticker and a B sticker, the degrees of conversion are sensitive to the sticker stoichiometry or the ratio of densities of stickers of A and B, $r = (c_A/s_A)/(c_B/s_B)$ (eq. A.16), highlighting that control over reversible bond formation can be achieved by adjusting the composition of the polymer mixture. A well-studied experimental example is how the degree of complexation of poly(vinyl alcohol) with molecular dye, Congo Red, can be tuned dependent on composition.[98,99] There is emerging evidence that the liquid–liquid phase separation of nucleic acids and proteins to form membraneless organelles in vivo is similarly sticker-stoichiometry controlled.[19,20]

Consider, more generally, the conversion degrees for any sticker stoichiometry, below the overlap of attractive volumes of stickers,

$$p_A \simeq \lambda \frac{c_B}{s_B} \quad \text{for} \quad \lambda \frac{c_A}{s_A} \ll 1 \tag{3.8}$$

and

$$p_B \simeq \lambda \frac{c_A}{s_A} \quad \text{for} \quad \lambda \frac{c_B}{s_B} \ll 1 \tag{3.9}$$

This again highlights that the fractional conversion of A, p_A, is the probability of an A sticker to be within the attractive volume of a B sticker, and vice versa.

Note that in this regime, the last three terms in the free energy density (eq. 2.4) related to sticker associations take the form of a pairwise attraction between stickers $-\lambda c_A c_B/(s_A s_B)\, k_{\mathrm{B}} T$. This pairwise attraction reduces the χ_{AB} parameter for $A-B$ interactions by the attractive volume per monomer, $(\lambda/a^3)/(s_A s_B)$,

$$\chi_{AB}^{\mathrm{eff}} = \chi_{AB} - \frac{\lambda/a^3}{s_A s_B} \tag{3.10}$$

where λ is the attractive volume of a bond ($\lambda = v_{\mathrm{b}} \exp(\epsilon)$) and $s_i = N_i/(f_i - 1)$ is the number of monomers between the neighboring stickers on chain type i. To determine the stability of the single phase in this low conversion regime (for $p_A, p_B \ll 1$) we can use the results for polymer mixtures by replacing χ_{AB} by χ_{AB}^{eff} (eq. 3.10). This implies that the physical associations between different species improve their mutual miscibility, a remarkable difference from $A-A$ homotypic associative polymers, where the physical associations reduced the stability of the single-phase solution by reducing the effective second virial coefficient: $v^{\mathrm{eff}} = v - \lambda/s_A^2$.[32] Importantly, this $A-B$ attraction stabilizes $A-B$ mixing, but also leads to $A-B$ gels separating from solution, as will be discussed in Section 5.

Above the overlap of attractive volumes of one (or both) sticker types, $\lambda c_A/s_A \gg 1$ or $\lambda c_B/s_B \gg 1$, the degrees of conversion depend on asymmetries in the number of stickers. For $r \ll 1$, A stickers are scarce and surrounded by an excess of available B stickers; p_A tends to unity as the attractive volumes of A approach overlap and nearly all the available A stickers are bound. On the contrary, for $r \gg 1$, A stickers are overabundant and there are not enough available B stickers with which to pair (all B stickers are paired, $p_B \approx 1$), and

13

the degree of conversion of A is reduced by a factor of the ratio of the number of stickers:

$$p_A \simeq \begin{cases} 1 & r \leq 1 \\ r^{-1} & r > 1 \end{cases} \quad \text{for} \quad \lambda \frac{c_A}{s_A} \gg 1 \tag{3.11}$$

Correspondingly,

$$p_B = r p_A \simeq \begin{cases} r & r < 1 \\ 1 & r \geq 1 \end{cases} \quad \text{for} \quad \lambda \frac{c_B}{s_B} \gg 1 \tag{3.12}$$

This has the remarkable consequence that even for infinitely strong association strengths, not all stickers will undergo cross-linking if there is an overabundance of those stickers (or deficiency of available sticker partners). Sticker number density asymmetries ($c_A/s_A \neq c_B/s_B$), arising from mismatched monomer concentrations for chains with the same number of monomers between stickers ($s_A = s_B$), or different densities of stickers per chain ($s_A \neq s_B$) at the same monomeric concentrations, significantly alter the degree of conversion (Figure 5).

This is perhaps most evident in the probability of paired stickers p_A relative to this probability $p_A(r = 1)$ for a sticker stoichiometric mixture (Figure 5b). For mixtures in which the A stickers are in short supply relative to the B stickers ($r \ll 1$), the enhancement at low binding ($\lambda c_A/s_A \ll 1$) is inversely proportional to their deficiency ($p_A/p_A(r = 1) \sim r^{-1}$, eq. 3.8). For a large attractive volume fraction of stickers, $\lambda c_A/s_A \gg 1$, the enhancement disappears as almost all A stickers become paired for $r \leq 1$. For mixtures in which the A stickers are in excess ($r \gg 1$), the degree of conversion p_A is nearly uniformly suppressed by a factor of r relative to the sticker stoichiometric mixture: $p_A/p_A(r = 1) \sim r^{-1}$. This is because the A stickers are overabundant relative to potential B sticker partners; their conversion is dominated across the range of attractive volume fraction of A stickers, $\lambda c_A/s_A$, by the stoichiometry of B.

However, a keen observer will notice the non-monotonicity of $p_A/p_A(r = 1)$ with $r > 1$ (Figure 5b). This melioration of the relative fractional degree of conversion occurs for
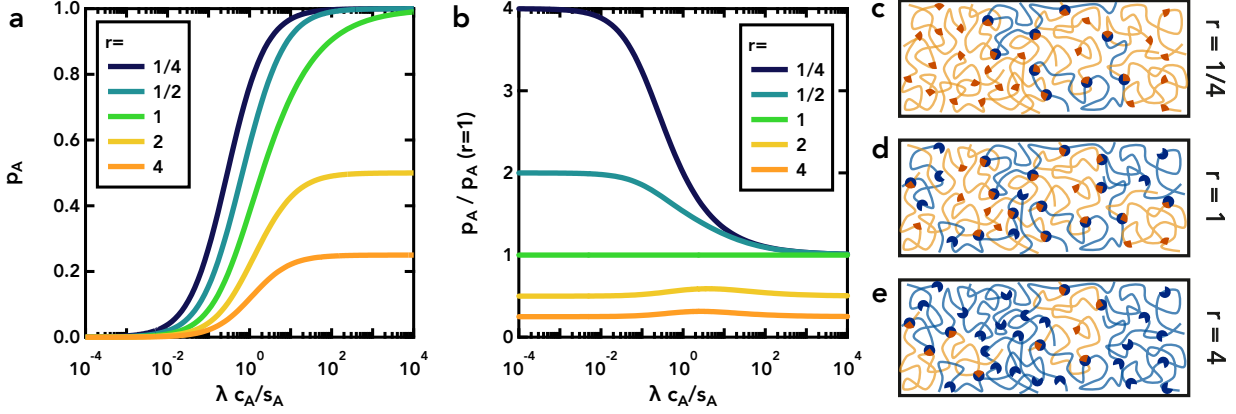
Figure 5: (a) Degree of conversion of A stickers, p_A, and (b) degree of conversion of A stickers relative to the degrees of conversion of the stoichiometric sticker mixture ($r = (c_A/s_A)/(c_B/s_B) = 1$) for a Θ-solution of associating polymers of type $A - B$ for various ratios r of A and B sticker concentrations as a function of increasing attractive volume fraction of A stickers $\lambda c_A/s_A$. (c-e) Schematic illustration of mixtures of $A - B$ associating polymers at different sticker stoichiometries, showing the effects of sticker stoichiometry on sticker degrees of conversion at high attractive volume fraction of A stickers $\lambda c_A/s_A \gg 1$. A stickers are denoted by blue major sectors and B stickers are denoted by orange minor sectors, as in Figure 3. Closed sticker pairs are indicated by the union of these blue and orange sectors.

intermediate attractive volume fraction of stickers (i.e., $\lambda c_A/s_A$ is of the order of unity) and is maximized at $r = 2$. It can be explained as follows: (1) at low $\lambda c_A/s_A$, below the overlap of attractive sticker volumes, most stickers are unpaired independent of the sticker stoichiometry asymmetry, but p_A increases for all r as $\lambda c_A/s_A$; (2) upon further increasing $\lambda c_A/s_A$, the attractive volumes of stickers overlap, most available B partners become paired, and this effect diminishes.

Ultimately, these effects are a consequence of the heterotypic nature of the reversible sticker association,

$$A + B \rightleftharpoons AB \tag{3.13}$$

which characterizes the ratio of bound to unbound stickers according to a mass action law,

$$K_{\text{eq}} = \frac{k_a}{k_d} = \frac{\rho}{\frac{c_A}{s_A}(1 - p_A)\frac{c_B}{s_B}(1 - p_B)} = \frac{p_A}{\frac{c_B}{s_B}(1 - p_A)(1 - p_B)} = \frac{p_B}{\frac{c_A}{s_A}(1 - p_A)(1 - p_B)} = \lambda \tag{3.14}$$

15

with an equilibrium constant K_{eq} and rate constants for association k_a and dissociation k_d. Accordingly, when A stickers are dilute in B (i.e., $r \ll 1$), the probability that A is paired increases with increasing availability of B (Figure 5a-c). Conversely, for $r \gg 1$, p_A is suppressed as the availability of free B stickers decreases (as $c_B/s_B = r^{-1}c_A/s_A$ decreases in Figure 5a,b,e). Most importantly, the equilibrium constant is simply what we have termed the attractive volume of a bond: $K_{\text{eq}} = \lambda$, and scales exponentially with the energy of association $\epsilon\, k_{\text{B}}T$.

In our mean-field theory, the probability of bound pair formation is unaffected by other interactions; it is purely statistical and is only weighted by the energy of the bond. The basic simplifying assumptions used in the description of condensation polymerization [41,42,44,100–104] and homotypic reversible associating polymers [32] are also adopted, namely: (a) all unreacted stickers of the same type are equally reactive and (b) all functional groups react independently. Consequently, our results depend on the sticker association being saturable (only two stickers can bind) with no local segregation of A and B, independent of the strength of associative interactions between stickers. Additionally, while on a monomeric level, sticker interactions are directional, we have assumed that this is averaged out on the scale of polymer chain segments relative to the size of the spacer, and there are no correlations or cooperativity between stickers, nor are the local chain conformations (e.g., persistence length) affected by the reversible bonds. Taking scaling corrections into account, we will see how the bound pair formation is affected by swelling in good solvents in a subsequent paper. Similar approaches could also be envisaged to consider sticker cooperativity and correlations.

4   Gelation

Our description of the sticker binding thus far has focused on the probability of an isolated sticker in mean-field forming a reversible bond. However, the stickers are distributed along polymer chains, so when a pair of stickers associates, a reversible cross-link is formed between

two polymers. In multifunctional polymers, i.e., polymers with many stickers, $f_i > 2$, the result of these associations is the formation of large, cross-linked clusters and ultimately percolation and formation of a connected network.

4.1 Gel Point

A convenient presentation of the mean-field model is to place the polymers on the vertices of an infinite Bethe lattice (Figure 6). Each vertex is connected with a functionality according to the number of stickers, f_i, and the bonds are formed with a probability, p_i. In such a bond percolation model, the probability of forming a bond is assumed to be independent of any other bonds in the system. Note that another assumption of the bond percolation model—the absence of intramolecular cross-linking, which had large implications for $A-A$ associations,[32] is less of a limitation for $A-B$ systems where all the associations are interchain. Since associations are only allowed between distinct species, the gels are *alternately cross-linked networks* between A chains and B chains. In a sense, these networks are branched and percolated block copolymers, in which the "block" size is the distance between cross-links (equal to the spacer length between stickers s_i for complete binding). In principle, each component could further have different monomeric sizes, solvent quality, etc.
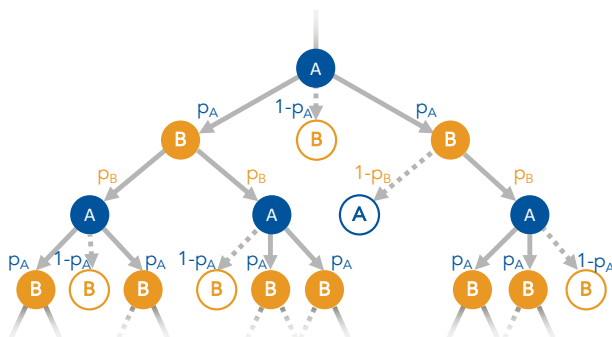

Figure 6: Gel point calculation on a Bethe lattice, visualized for $f_A = 4$ and $f_B = 3$. Filled circles correspond to stickers attached to the Cayley tree; unfilled circles are not attached. Solid grey lines indicate formed bonds with probabilities p_A and p_B; dashed lines indicate bonds not formed with probabilities $1 - p_A$ and $1 - p_B$. The fractional degrees of conversion are related according to the stoichiometry of stickers: $p_B = r p_A$.

As was shown for $A - A$ associating polymers in Ref. 32, the gelation conditions can be obtained according to the Bethe lattice description as in Figure 6. The gelation condition corresponds to the product of the degrees of conversion of both A and B:[44,66,71,76,101,103,104]

$$p_A^{\text{gel}} p_B^{\text{gel}} = r \left(p_A^{\text{gel}} \right)^2 = \frac{1}{f_A - 1} \frac{1}{f_B - 1} \tag{4.1}$$

which corresponds to a critical degree of conversion of A:

$$p_A^{\text{gel}} = \frac{1}{\sqrt{r (f_A - 1) (f_B - 1)}}. \tag{4.2}$$

The result is consistent with the classical gelation theory of Flory and Stockmayer in the pre-gel regime.[41–44] In the post-gel regime, the present theory is compatible with the Flory model,[44] implying that finite clusters and the reversible gel are not restricted to tree-like structures but should contain cycles.

It follows that the attractive volume of a bond for the critical gel (i.e., the equilibrium constant for reversible heteroleptic association, eq. 3.14) results from evaluating eq. A.13 at the critical degrees of conversion:

$$\lambda^{\text{gel}} = \frac{p_A^{\text{gel}}}{\frac{c_B}{s_B} \left(1 - p_A^{\text{gel}} \right) \left(1 - p_B^{\text{gel}} \right)} = \frac{p_B^{\text{gel}}}{\frac{c_A}{s_A} \left(1 - p_A^{\text{gel}} \right) \left(1 - p_B^{\text{gel}} \right)} \tag{4.3}$$

which can be simply approximated in the limit of many stickers per chain:

$$\lambda^{\text{gel}} \simeq \frac{1}{\frac{c_B}{s_B} \sqrt{r} \sqrt{f_A f_B}} = \frac{\sqrt{r}}{\frac{c_A}{s_A} \sqrt{f_A f_B}} \quad \text{for } f_A, f_B \gg 1 \tag{4.4}$$

The critical gelation concentration of stickers A and B, i.e., $\frac{c_A}{s_A} + \frac{c_B}{s_B} = \frac{c_B}{s_B}(1 + r)$, can be analogously determined from eq. A.13 at p_A^{gel} (eq. 4.2):

$$\left(\frac{c_A}{s_A} + \frac{c_B}{s_B} \right)^{\text{gel}} = \frac{p_A^{\text{gel}}(1 + r)}{(1 - p_A^{\text{gel}})(1 - r p_A^{\text{gel}})\lambda} \tag{4.5}$$

which also simplifies in the limit of many stickers per chain:

$$\left(\frac{c_A}{s_A} + \frac{c_B}{s_B}\right)^{\text{gel}} \simeq \frac{1+r}{\lambda\sqrt{r}\sqrt{f_A f_B}} \quad \text{for } f_A, f_B \gg 1 \tag{4.6}$$

In the symmetric case ($\frac{c_A}{s_A} = \frac{c_B}{s_B}$, $f_A = f_B$), the pairwise associative nature results in a total gelation concentration that is twice the gelation concentration for $A - A$ associative polymers at the same λ and f_A. This doubling of the gelation concentration is due to the alternating nature of the cross-links and the need for both A and B to participate in the gelation. However, more importantly, the gel condition of eq. 4.6, considered as an equation for r has two roots corresponding to $r < 1$ and $r > 1$. Thus, there exist two critical gelation composition asymmetries for a specified overall concentration of stickers.

4.2   Re-entrant Sol–Gel–Sol Transition

The gelation conditions (either eq. 4.3 or eq. 4.5) in reversible networks of $A - B$ associating polymers result from the hetero-complementary nature of bond formation, with an important implication—a sol–gel–sol or re-entrant gelation transition. Gelation can only proceed in a region of composition space with adequate number densities of both A and B stickers to maintain bond percolation; if either species is present in high enough excess ($r \ll 1, \gg 1$), infinite networks will not be formed (Figure 7), even at strong binding conditions with all the minority sticker bonded.

Figure 7 shows this re-entrant gelation transition as embodied by the λ necessary for gelation as a function of sticker stoichiometry r at different total concentrations. Conceptually, this emphasizes that the critical energy of association for gelation increases at fixed $c_A + c_B$ as the ratio of sticker concentrations deviate from stoichiometry. At $r = 1$, the
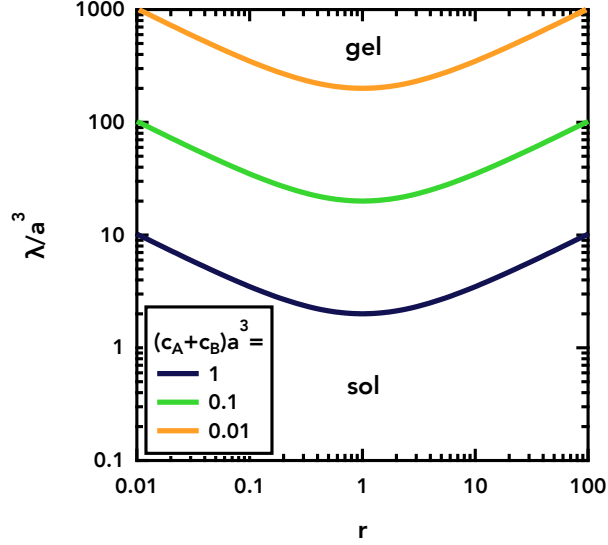
Figure 7: Gel conditions highlighting the re-entrant sol–gel–sol transition at fixed total volume fractions ($(c_A + c_B)a^3 = 0.01, 0.1, 1$) as a function of sticker stoichiometry, r, for polymers with spacers containing $s_A = s_B = 1000$ monomers, $f_A = f_B = 1000$ stickers, and degrees of polymerization $N_A = N_B = 10^6$.

minimum association strength for gelation is reciprocally proportional to $c_A/s_A + c_B/s_B$:

$$\lambda^{\text{gel}}(r = 1) = \frac{2\sqrt{f_A - 1}\sqrt{f_B - 1}}{(\sqrt{f_A - 1}\sqrt{f_B - 1} - 1)^2 \left(\frac{c_A}{s_A} + \frac{c_B}{s_B}\right)} \tag{4.7}$$

$$\simeq \frac{2}{\sqrt{f_A f_B}\left(\frac{c_A}{s_A} + \frac{c_B}{s_B}\right)} \quad \text{for } f_A, f_B \gg 1 \tag{4.8}$$

For arbitrary sticker composition, the factor of 2 in eq. 4.8 must be replaced with $\sqrt{r} + 1/\sqrt{r}$:

$$\lambda^{\text{gel}} \simeq \frac{\sqrt{r} + 1/\sqrt{r}}{\sqrt{f_A f_B}\left(\frac{c_A}{s_A} + \frac{c_B}{s_B}\right)} \quad \text{for } f_A, f_B \gg 1 \tag{4.9}$$

At sticker concentrations away from stoichiometry, λ^{gel} increases proportionally to $\sqrt{r}$ with increasing r for $r \gg 1$ and proportional to $1/\sqrt{r}$ with decreasing r for $r \ll 1$. At a constant λ (i.e., a constant temperature), the system is a sol, gels, and then returns to a sol phase as the ratio r of the number of A to B stickers increases. Accordingly, this sol–gel–sol re-entrant phases can be described as a mixture of hetero-associating polymers with an excess

of B stickers for small r and few bound $A - B$ pairs which transform (as r increases) to a fully percolated network with many associations, and, ultimately to a mixture of hetero-associating polymers with an excess of A stickers and few bound $A - B$ pairs for large r. This reiterates the importance of the sticker stoichiometry in determining the binding statistics, as shown schematically in Figure 5c-e.

Signatures of this re-entrant sol–gel–sol transition have been observed in solutions or blends of hetero-associating polymers through a peak in shear modulus or viscosity at near-stoichiometric mixing conditions. For example, a gelatin solution exhibited a non-monotonic increase then decrease in the storage modulus upon addition of sodium polystyrene sulfonate (NaPSS).[105] Light scattering of dilute NaPSS–gelatin mixtures correlated the maxima in the apparent molecular weight with the same composition ratio as the peak in shear modulus, confirming that the re-entrant gelation transition corresponded to the 1:1 stoichiometry of the ionic binding sites between NaPSS and gelatin.[105,106] The viscosity of mixtures of polysaccharides have also been shown to vary non-monotonically with composition.[107] At concentrations with similar viscosities in pure solutions of dextran and κ-carrageenan, binary mixtures show a pronounced viscosity increase (by a factor of 3) at intermediate mixing ratios.[107] While the reported relative viscosity increases are statistically above expectations from a logarithmic mixing rule, they are perhaps lower than the orders of magnitude increase that might be possible due to the re-entrant sol–gel–sol transition.

A significant challenge is that many experimental systems are complicated by numerous other factors and do not necessarily provide an appropriate means to test the predictions. For example, gelatin alone reversibly cross-links by triple helix formation and polysaccharide solutions interact by multiple associative interactions that are composition and solvent-dependent, convoluting the experimental observations. More idealized systems of binary hetero-complementary associative polymers based on cyclodextrin inclusion compounds have since been reported to show a significant viscosity increase at stoichiometric binding conditions.[54] If the self-associative interactions are suppressed, this system exhibits

a sol–gel–sol transition as the stoichiometry of stickers is altered, with a reported several orders of magnitude increase in the shear modulus at stoichiometric ($r = 1$) mixing.[55,108,109]

Another complication in the quantitative analysis of sol–gel–sol re-entrant transitions is the propensity for phase separation at equal mixing conditions into a dense phase with high viscosity/modulus and a more dilute phase,[109] as discussed in more detail in Section 5. This is often discussed in the context of coacervation, particularly the complexation of two oppositely charged polyelectrolytes.[77,110,111]

4.3 Stimuli-Responsive Associations

There is another emerging area where these sol–gel–sol re-entrant transitions commonly occur—polymers with stimuli-responsive associations. In this case, the number of stickers of A and B can be altered by external stimuli, without changing the overall polymer concentrations. This has the remarkable consequence, that the re-entrant gelation transition described above should also be accessible in a single solution (or blend) of hetero-associative polymers if the binding propensity of the stickers can be controllably varied.

Consider a simple example of a mixture of weak polycations and weak polyanions in aqueous solution. If, for simplicity, the oppositely charged polyelectrolytes have a common $pK = pKa$ and an equal number of ionizable moieties per chain, then the total numbers of stickers is constant, $f_A + f_B$ = constant. At the pH corresponding to their pK, both polyelectrolytes have the same number of charges and thus the same number of stickers, $f_A = f_B$. Farther away from their pK, at either low or high pH, only one of the polyelectrolytes is highly charged (has many stickers), while the other becomes depleted in charges (stickers). In this example, at high or low pH, the stickers of the two chains are strongly non-stoichiometric but are in stoichiometric proportions when the pH of the solution is at the common pK. This leads to a similar sol–gel–sol transition to that described in Section 4.2. Here, the sol–gel–sol transition is ascribed to the continuous transition from non-percolating clusters to a fully percolated network back to non-percolating clusters as the sticker stoichiometry is altered

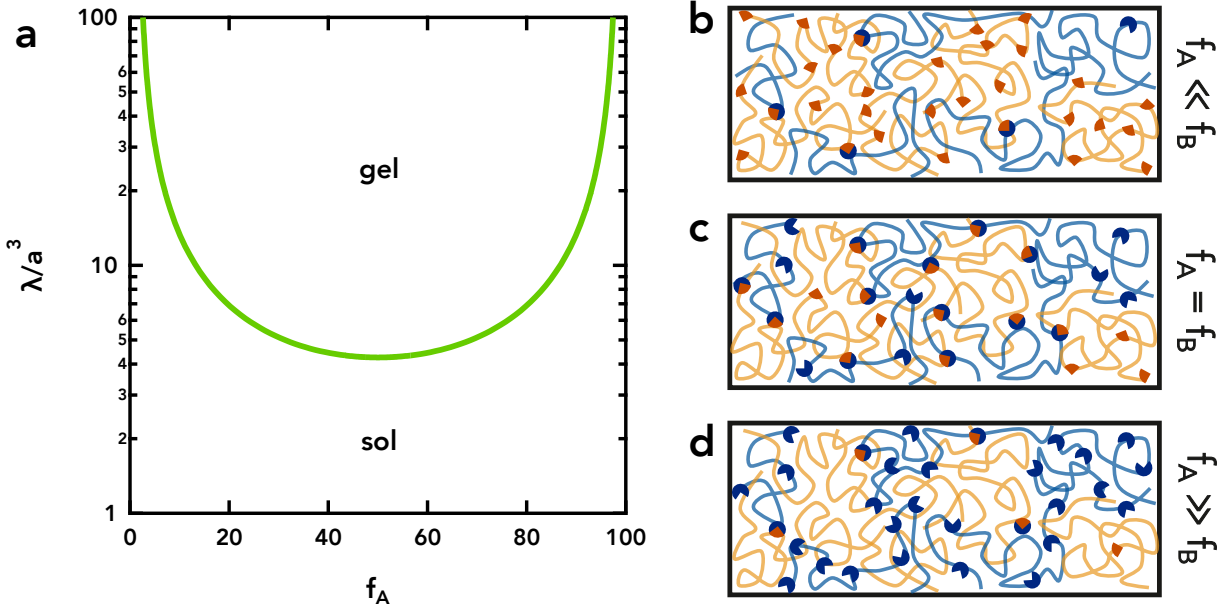from low to high pH across the common pK (Figure 8).

Figure 8: The stimuli-responsive sol–gel–sol re-entrant transition as a function of the number of A-stickers, f_A, for $N_A = N_B = 1000$, $c_A a^3 = c_B a^3 = 0.1$, and $f_A + f_B = 100$. This regime can be realized, for example, by adjusting pH in the vicinity of the common $pK = pKa$ of both polyelectrolytes, for $\lambda/a^3 > 5$. A stickers are denoted by blue major sectors and B stickers are denoted by orange minor sectors, as in Figure 3. Closed sticker pairs are indicated by the union of these blue and orange sectors.

Subsequently, such a stimuli-responsive sol–gel–sol transformation would result in a non-monotonic, bell-shaped variation of viscoelasticity versus pH (or another stimulus). This would impart the ability to selectively thicken an aqueous solution within a narrow pH response range, providing the potential for tunable drug release or delivery rates.[112] This is commonly used as a method of encapsulation in the food and pharmaceutical industries, and as the basis for many forms of biomolecular condensates in the cell.[113–118] Associating biomacromolecules can also be tuned by addition and removal of a target biomolecule stimulus, such as a biotinylated polymer in the presence of avidin.[119]

Other more complicated examples exist of stimuli-responsive sol–gel–sol re-entrant transitions, such as that of multiblock poloxamer solutions, wherein the polymer solubility and degree of ionization are altered with pH.[120] Furthermore, as the pH (or other stimulus) is

changed, the relationship between f_A and f_B does not need to be inversely correlated as shown in Figure 8. More complicated relationships can be envisaged and would result in different shapes of the re-entrant gelation transition boundary with respect to stimulus or composition.

The described connectivity transition occurring at the gel point is incredibly important in the dynamics of associative polymers. Yet, importantly, gelation is not a thermodynamic transition, the free energy density and all derivatives are perfectly analytical at the gel point, as we will see in the next section.

5 Phase Behavior

The associative interactions that drive gelation can also cause phase separation. The phase behavior of the system can be analyzed in a standard way through thermodynamic operators derived from the free energy (Appendix A), ensuring mechanical ($\Pi^I = \Pi^{II}$) and chemical ($\mu_i^I = \mu_i^{II}$) equilibrium.

5.1 Sticker-Stoichiometric Mixtures

Consider the phase behavior of sticker-stoichiometric mixtures of hetero-complementary associating polymers, with $c_A/s_A = c_B/s_B$, and compare their phase diagram with a comparable homotypic associating system. Figure 9 shows the phase diagrams of solutions of homo- and hetero-associating polymers in a common Θ solvent in the plane of total polymer concentration–attractive volume of a bond λ. For a direct comparison, we show a spacer-symmetric ($s_A = s_B$), sticker-stoichiometric $A - B$ mixture ($r = 1$, $c_A/s_A = c_B/s_B$).

The phase-coexistence boundary at stoichiometric conditions ($c_A/s_A = c_B/s_B$) has the same functional form as for $A - A$ associative polymers, with only an increase in the critical attractive volume of a bond (Figure 9). For $A-A$ associating polymers, this critical attractive volume of a bond is $\lambda_{\mathrm{cr}} \simeq s_A^2 \left(v + 2\sqrt{w/N_A} \right)$.[32] In the sticker-stoichiometric case of $A - B$
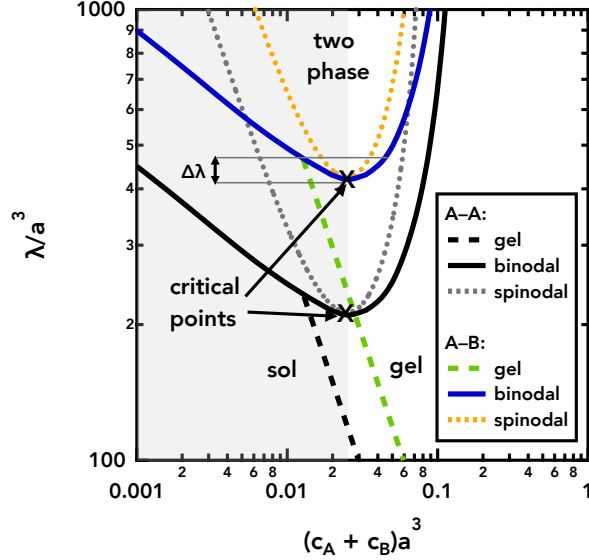
Figure 9: Phase diagram of a Θ-solution of associating polymers of type $A - B$ for $f_A = f_B = 20$, $s_A = s_B = 50$, $N_A = N_B = 1000$ and $v = 0$, $w = a^6$, $\chi_{AB} = 0$ for stoichiometric $c_A = c_B$ presented against comparable $A - A$ system with $f = 20$, $s = 50$, $N = 1000$, $v = 0$, and $w = a^6$. Light grey shaded region is outside the applicability of the mean-field theories, $c < c^*$.

associating polymer mixtures with $r = 1$, this critical point is increased to higher association strengths by a factor of two (or, more generally, of approximately $\sqrt{r} + 1/\sqrt{r}$ for any r), corresponding to identical degrees of conversion at the critical transition ($p_A(A - A) = p_A(A - B)$ at λ_{cr} and $c_{\mathrm{cr}} = (c_A + c_B)_{\mathrm{cr}}$.

If λ is small, such that $\lambda < \lambda_{\mathrm{cr}}$, then the solution is stable; the system does not phase separate. For higher association strengths, $\lambda > \lambda_{\mathrm{cr}}$, the solution can phase separate into dilute and concentrated phases. While outside the applicability of the described mean-field theory, the concentration of the dilute phase should rapidly decrease with increasing λ, becoming exponentially low. In the dilute phase, the polymers are isolated coils at low $\lambda < \lambda_{\mathrm{cr}}$, but with higher bond energies ($\lambda > \lambda_{\mathrm{cr}}$), strong attraction between stickers would promote complexes with aggregation number depending on the asymmetry in the number of stickers-per-chain f_A/f_B. The density inside these complexes is higher than the mean density inside unperturbed chains and is dictated by the balance of three-body repulsion and entropy associated with different bridging combinations. Unlike globule formation in

25

solutions of homo-associating A chains, hetero-associating mixtures of A and B chains require a minimum of two chains (one each of A and B for a symmetric mixture with $f_A = f_B$) to form a well-defined complex. Higher aggregation numbers than two are possible (especially for large asymmetries in the functionalities $f_A \gg f_B$ or $f_B \gg f_A$), depending on the balance of the energy of unsaturated stickers in the complex and the larger reduction in translational entropy compared to dimers. In the dense phase, the concentration approaches a constant at high λ,

$$c_A = c_B \simeq \frac{1}{2}\sqrt{\frac{3}{2ws_A}} \simeq \frac{1}{2}\sqrt{\frac{3}{2ws_B}} \tag{5.1}$$

limited by repulsion between polymer strands (excluded volume interactions in good solvent and three-body repulsions in the Θ-regime considered here).

For most solution conditions (away from the critical point, at $\lambda \gg \lambda_{cr}$), phase separation results in a dilute sol phase in coexistence with a highly connected dense gel phase (with $p_A = p_B$ close to 1). For excluded volume parameters $v \geq 0$, the critical point always corresponds to the gel state, and sol–sol phase separation is not possible at any λ. This is because except for possible poor solvent conditions, the only attractions driving coacervation are the sticker bonds also driving gelation. Interestingly, however, near the critical point, both the polymer-poor and polymer-rich phases are reversible networks.

Accordingly, there is a narrow range of concentrations and association strengths where gel–gel phase separation should be seen, in both $A - A$ and $A - B$-type associating polymer mixtures. The loosely connected gel could be expected to have nearly ideal chain conformations with fewer cross-links, while the dense gel would be interpenetrating with many cross-links. The coexisting gels differ in composition, not only concentration, but for overall non-stoichiometric mixtures, the denser gel is also more sticker stoichiometric, with more associations. The width of this gel–gel coexistence window (either $\Delta\lambda/\lambda$ or $\Delta(c_A + c_B)a^3$) is independent of the density and absolute number of stickers per chain. Instead, at the mean-field level, this region is seemingly universal, dependent only on the critical behavior. Such a gel–gel phase separation has been recently reported in hetero-binding tetra-arm

26

poly(ethylene glycol) stars.[121] More systematic studies are needed to understand the conditions of gel–gel phase coexistence and resultant structures and dynamics. However, it should be noted that, in this window, close to both the critical and gel points, compositional fluctuations are large and highly inhomogeneous (turbid) networks might be more commonly observed experimentally.

5.2 Non-Stoichiometric Mixtures

Thus far, we have only shown the phase diagram for a mixture of hetero-complementary associating chains in the sticker-stoichiometric case ($r = 1$, Figure 9). Importantly, however, since the sticker degrees of conversion are sensitive to the ratio of densities of stickers of A and B, as discussed in Section 3.2, so is the phase behavior. In our system, we consider an incompressible ternary mixture of A and B polymers in solvent, in which it is convenient to present the compositional dependence of the phase behavior as quasi-two component with the solvent concentration implicit. We can more fully reflect this two-component phase equilibrium—polymers A and B (with implicit solvent)—as a three-dimensional phase diagram of compositional axes versus binding strength (Figure 10a). Logarithmic compositional axes emphasize key effects for dilute and strongly non-stoichiometric mixtures, while the logarithmic axis for the association strength (as characterized by the attractive volume of a bond, λ) reflects the sensitivity of phase behavior to the binding energy.

It is instructive to focus attention on the compositional dependence of our $A - B$ heterobonding mixture. Figure 10b presents a cut of the full three-dimensional phase diagram of heterotypic associating A and B polymers at a specific $\lambda/a^3 = 250$ as a function of monomeric concentrations c_A and c_B. The binodal and spinodal conditions demarcating the phase stability are shown in Figure 10b, along with representative tie lines between co-existing compositions.

The two-phase region exists at low to intermediate monomeric concentrations (centered near the overlap concentration, $c \sim c^*$) and is largest at sticker stoichiometric conditions
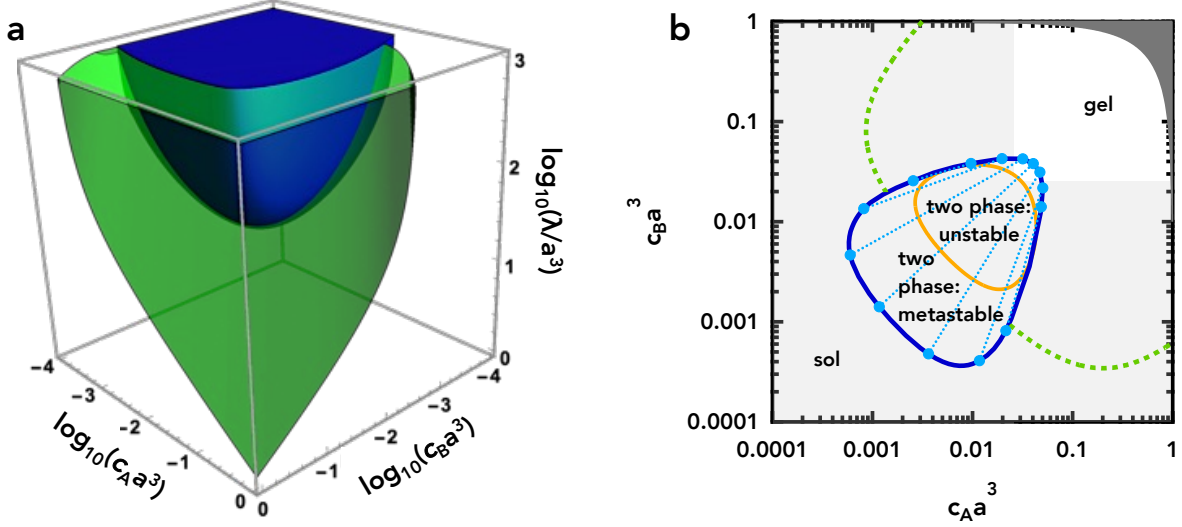
Figure 10: Phase diagram of a Θ-solution of associating polymers of type $A - B$ for $f_A = 20$, $f_B = 50$, $s_A = 50$, $s_B = 20$, $N_A = N_B = 1000$, $v = 0$, $w = a^6$, and $\chi_{AB} = 0$: (a) full three-dimensional phase diagram with a two-phase region (binodal) in dark blue and gel region in green; and, (b) cut of phase diagram at $\lambda/a^3 = 250$. Tie lines (light blue dotted lines) highlighting the partitioning between the dilute and concentrated phases are shown for the two-phase region (binodal in dark blue, spinodal in orange). The boundary of the gel region is marked by the dashed green line. Dark grey shaded regions are inaccessible due to incompressibility. Light grey shaded regions are outside the applicability of the mean-field theory, $c < c^*$.

$(r = 1, c_A/s_A = c_B/s_B)$. This is because the macroscopic phase separation is a result of the associations between stickers, which are maximized at stoichiometry. From the tie lines, it is apparent that the phase separation results in a dilute phase in coexistence with a dense, more symmetric gel phase. This behavior has been observed in the case of interchain ion–dipole interactions in polyamide/ionomer blends,[122,123] cation–π interactions in like-charged poly-electrolytes,[56] and the coacervation of oppositely charged polyelectrolytes.[77,124–127]

Upon mismatch in the number densities of stickers, $c_A/s_A \neq c_B/s_B$ or $r \neq 1$, the excess stickers are expelled to the less dense phase. Much like the sticker-stoichiometric case, it is expected that at high λ, the dilute phase ($c < c^*$) will consist primarily of globular complexes of a finite number of associated chains, although this is outside the applicability of the described mean-field theory.

Given the mismatch in the number densities of stickers A and B, not all the stickers

will be paired. The excess free stickers may exist within aggregates of multiple chains or on free chains, depending on the balance of chain translational entropy, excluded volume interactions, and sticker association energy. In the absence of electrostatic or other long-range interactions, the complexes are expected to form "loopy" structures that optimize sticker binding with the Gaussian chain conformations of spacers between stickers. In the presence of un-screened charges, these complexes could form tadpoles, micelles, and more exotic geometries to expel the extra like charges away from the complex or globule.[84,128–132] Particularly at high association strengths, this phase separation could be harnessed to robustly produce well-formed gels, with nearly stoichiometric numbers of stickers of A and B, by mixing less concentrated solutions of A and B, without the need to be precisely at matched sticker concentrations. Further, the compositional dependence of the phase separation in Figure 10b highlights that the two phase region can be avoided, if desired, by controlling the composition to be too strongly asymmetric for coacervation during processing of the mixture. Or, as has been recently shown regarding cytoskeleton formation, the compositional dependence can also be used to control the growth and dissolution of membraneless organelles, by manipulation of the composition in and out of the unstable region.[133]

For illustration, in Figure 10, the phase behavior is shown for a mixture of multifunctional polymers with different densities of stickers per chain, $s_A \neq s_B$, causing the two phase region to appear asymmetric, tilted towards lower c_B, due to the higher density of stickers on B chains relative to A chains, $s_B < s_A$. The binodal and spinodal regions would appear symmetric with respect to the sticker number densities c_A/s_A and c_B/s_B, at equal degrees of polymerization $N_A = N_B$ or in the long chain limit $(N_A, N_B \to \infty)$. Importantly, this emphasizes that sticker–sticker attractions are responsible for driving phase separation, but translational entropy and short-range repulsions (two- and three-body contacts) between all monomers are responsible for stabilization.

This agrees well with beyond mean-field theoretical predictions of coacervates formed from charge-density-asymmetric mixtures of polyelectrolytes, in which the asymmetry in

spacer length between stickers was found to drive novel solution structures with unique mechanical signatures.[85,86,134] Although we have explicitly considered mild asymmetries in sticker number and densities between A and B, where both chains are polymeric with many stickers and spacers per chain, it remains an interesting problem for dynamics to consider highly asymmetric mixtures (e.g., metal–ligand associations[51,135–138] or small covalent adaptable cross-linkers.)[139–142] This is in part because the gelation boundary depends on the absolute number (not just density) of stickers per chain (eq. 4.5), becoming symmetric only for $f_A = f_B$ and $s_A = s_B$ (equivalently $N_A = N_B$) and not just $c_A/s_A = c_B/s_B$.

5.3 Chemical Incompatibility

A subtle feature of $A-B$ pairwise associations, visible in the Bethe lattice description (Figure 6), is that since cross-links are only allowed between different species—clusters (of finite or infinite size) are then effectively multiblock copolymers. For small degrees of chemical incompatibility between the varied species,

$$\chi_{AB} \ll \lambda/(s_A s_B a^3) \tag{5.2}$$

the present theory will be applicable. For larger segregation strengths, the effects of such chemical incompatibility between A and B associative polymers on the thermodynamics, percolation conditions, and structure formation may be significant and are investigated in a companion work, exploring a weak inhomogeneity expansion of the mean-field theory.[143]

The chemical incompatibility between polymers of type A and B drives a competition between associative and segregative phase separation. The addition of reversible $A - B$ cross-links between incompatible A and B chains compatibilizes the mixture, minimizing the propensity for macroscopic phase separation into A- and B-rich phases. However, under strong binding and segregation conditions, this results in eutectic-like behavior and local microphase segregation. The resultant microdomain structure can be tuned by the association

and segregation strengths, concentration, and spacer size between stickers.

5.4   Associations in Good Solvents

The mean-field model discussed above is not directly applicable to good solvents, for

$$v > a^3/\sqrt{N_i} \tag{5.3}$$

where the chain statistics are non-Gaussian, nor for higher values of the excluded volume parameter,

$$v > a^3/\sqrt{s_i} \tag{5.4}$$

where the spacers are swollen, and the probability of sticker contact is reduced. Thus, it becomes imperative to correctly account for the excluded volume interactions in swelling the chains and reducing the probability of contact between two stickers. We will report in a subsequent paper a scaling estimate that extends the current model for $A - B$ associative polymers to good solvents. The chain swelling decreases the overlap concentration, but the additional local repulsions also reduce $A - B$ interpenetration and thus the probability of sticker contact, particularly at low attractive volume fractions of stickers. The primary consequences are shifting the gelation transition to higher concentrations and the suppression of phase separation.

6   Conclusions

We have considered a mixture of a complementary pair of multifunctional heterobonding polymers A and B. The aim was to study the reversible network formation and phase behavior of hetero-associating polymer mixtures by extending an equilibrium statistical mechanical theory for the thermodynamics and gelation of associative polymers[32] to heterotypic $A - B$ interactions. Within this mean-field model, we have derived explicit analytical expressions

for the binding statistics, gelation condition, and free energy, permitting the quantitative calculation of gelation and phase boundaries. It is demonstrated that reversibly associating polymers have a large parameter space in terms of molecular design, binding energy, and mixture compositions.

Reversible binding between A and B stickers on different chains result in branched block copolymers and the formation of multi-component copolymer networks. Since the $A - B$ reversible bonds require both A and B associative groups, bond formation is maximized at sticker-stoichiometric conditions. This results in stabilization of the homogeneous gel phase at stoichiometry, and subsequently, a re-entrant sol–gel–sol transition as the composition is varied at concentrations above the gelation concentration. Stimuli-responsive multifunctional polymers, such as weak acids and bases whose charge (and thus, number of stickers) is pH-dependent, can also exhibit a sol–gel–sol transition as the stimulus rather than overall composition is varied. These predicted re-entrant gelation transitions appear to be well-supported by experiments on solutions of weak polyelectrolytes, polysaccharides, and host–guest inclusion compounds.[54,55,77,105–111]

However, it is shown that the association and reversible network formation are always accompanied by the tendency for phase separation. For weak attraction between stickers, the system is homogeneous at all concentrations, and a physical network is formed above the gelation concentration. The result is continuous gelation, from an overlapping $(c_A, c_B > c^*)$ sol to a reversible gel. For stronger attraction between stickers, the system undergoes discontinuous gelation, in which it becomes unstable over a wide concentration range, separating into a dense, symmetric gel in coexistence with a less concentrated phase. Close to the critical point for phase separation, a narrow window of gel–gel phase coexistence is also possible. In hetero-associating mixtures, the transition from discontinuous to continuous gelation and thus, whether the system phase separates, is also controllable by the relative compositions of A and B.

Although there are numerous reports of reversible network formation in mixtures of

hetero-complementary associating polymers, we are unaware of any experiments that have systematically explored the phase behavior. Although our model is not directly applicable to complexation from long-range interactions, experiments on coacervation formation in mixtures of polyelectrolytes at strong binding, however, appear qualitatively consistent with this work. Predictions of gelation and phase boundaries should be accessible by preparing mixtures of suitable heterotypic associating polymers at different concentrations. Our predictions are expected to be useful in the rational design of interacting polymer mixtures and the formation of reversible networks. Inclusion of chain connectivity and long-range interactions, including electrostatics, would help to bridge this general theory with those developed for polyelectrolyte complexation. Future work seeks to develop dynamical predictions based on the mean-field model presented.

Acknowledgement

A Mean-Field Theory

As a minimal model system, consider a solution of linear chains with associating groups (stickers) of type $i = A, B$ (Figure 3). Each chain of length N_i contains f_i stickers separated by spacers with $s_i = N_i/(f_i - 1)$ monomers, such that $f_i \ll N_i$ and thus $s_i \gg 1$. Since we consider sticky associations at the mean-field level without correlations, the specific distribution of stickers along the chain does not affect the thermodynamics. Stickers can associate in saturable $A - B$ pairs with the energy of association equal to $\epsilon\, k_{\mathrm{B}}T$, where $k_{\mathrm{B}}T$ is the thermal energy. The monomer concentration of type $i = A, B$ in solution is c_i, the number density of polymer chains is c_i/N_i, and the number density of stickers is $f_i c_i/N_i \simeq c_i/s_i$. The number of stickers in volume V is

$$N_{\mathrm{st},i} = f_i \frac{c_i}{N_i} V \simeq \frac{c_i}{s_i} V \tag{A.1}$$

Let p_i be the fraction (probability) of stickers of type i that are associated in a bound $A - B$ pair (i.e., the degree of conversion of type i). The number of such pairs of associated stickers is,

$$N_{\mathrm{p}} = p_i N_{\mathrm{st},i} \tag{A.2}$$

Thus, the density of temporary bonds (pairs of stickers) is

$$\rho = \frac{N_{\mathrm{p}}}{V} = p_i \frac{f_i c_i}{N_i} \simeq p_i \frac{c_i}{s_i} \tag{A.3}$$

The free energy density of a solution of A and B-type polymers with $A - B$ pairwise associations can be divided into three parts—translational free energy F_{tr} from the entropic mixing of polymer chains, F_{int} from the effective interactions between all monomers (both stickers and non-stickers) mediated by solvent, and the contribution F_{st} from sticker interactions:

$$F = F_{\mathrm{tr}} + F_{\mathrm{int}} + F_{\mathrm{st}} \tag{A.4}$$

The purely entropic contribution F_{tr} accounts for the translational entropy for a solution mixture of non-interacting polymers,

$$\frac{F_{\text{tr}}}{k_{\text{B}}T} = -\frac{1}{V}\ln Z_{\text{ref}} = \frac{c_A}{N_A}\ln\left(c_A a^3\right) + \frac{c_B}{N_B}\ln\left(c_B a^3\right) \tag{A.5}$$

The interaction part F_{int} can be written in terms of two- and three-body solvent-mediated interactions between monomers, as well as $A - B$ chemical incompatibility,

$$\frac{F_{\text{int}}}{k_{\text{B}}T} = \frac{v}{2}(c_A + c_B)^2 + \frac{w}{6}(c_A + c_B)^3 + \chi_{AB}a^3 c_A c_B \tag{A.6}$$

where v is the excluded volume parameter describing the solvent quality for both polymers, w is the three-body interaction parameter, and χ_{AB} is the direct Flory–Huggins interaction parameter between A and B monomers beyond the solvent-mediated contributions that are included in the $v c_A c_B$ term. We consider identical two- and three-body interactions between A and B chains with the same v and w for all monomers.

To calculate the free energy density due to the association of stickers, F_{st}, we stipulate that N_{p} stickers of A and N_{p} stickers of B form N_{p} bonds. The contribution of bonds to the partition function is

$$Z_{\text{st}} = P_{\text{comb}} W \exp\left(\epsilon N_{\text{p}}\right) \tag{A.7}$$

where P_{comb} is the number of separate ways to choose N_p $A - B$ pairs of stickers from $N_{\text{st},A}$ A stickers and $N_{\text{st},B}$ B stickers. W is the probability that all chosen stickers, in the absence of attractive interactions, can be found close enough to their partners to form bonds:

$$W = \left(\frac{v_{\text{b}}}{V}\right)^{N_{\text{p}}} \tag{A.8}$$

where v_{b} is the bond volume. The number of separate ways of selecting N_{p} stickers from a

total number $N_{\text{st},i}$ of stickers of type i is a binomial coefficient,

$$\frac{N_{\text{st},i}!}{(N_{\text{st},i} - N_{\text{p}})! N_{\text{p}}!} \tag{A.9}$$

and the number of separate ways to pair N_{p} A stickers and N_{p} B stickers is simply $N_{\text{p}}!$. Therefore, the combinatorial factor is

$$P_{\text{comb}} = \frac{N_{\text{st},A}! N_{\text{st},B}!}{(N_{\text{st},A} - N_{\text{p}})! (N_{\text{st},B} - N_{\text{p}})! N_{\text{p}}!}. \tag{A.10}$$

Thus, the part of the free energy density due to stickers is

$$\frac{F_{\text{st}}}{k_{\text{B}}T} = -\frac{1}{V} \ln\left(Z_{\text{st}}\right) = \frac{c_A}{s_A}\left(1 - p_A\right)\ln\left(1 - p_A\right) + \frac{c_B}{s_B}\left(1 - p_B\right)\ln\left(1 - p_B\right)$$

$$+ \rho\left[1 - \epsilon + \ln\frac{\rho s_A s_B}{c_A c_B v_{\text{b}}}\right] \tag{A.11}$$

where the first two terms correspond to the entropy of the unpaired A and B stickers and the final terms correspond to the energy of the paired stickers including their enthalpy of association ($\epsilon\rho$) and their entropy change from bonding ($\rho[1 + \ln\frac{\rho s_A s_B}{c_A c_B v_{\text{b}}}]$).

The total free energy density $F = F_{\text{tr}} + F_{\text{int}} + F_{\text{st}}$ should be minimized with respect to the density of temporary bonds ρ, or similarly, with respect to the degrees of conversion. The condition for the free-energy minimum is

$$\frac{p_A}{\left(1 - p_A\right)\left(1 - p_B\right)} = \frac{c_B}{s_B} v_{\text{b}} \exp\left(\epsilon\right) \tag{A.12}$$

or equivalently

$$\lambda = \frac{p_A}{\frac{c_B}{s_B}\left(1 - p_A\right)\left(1 - p_B\right)} = \frac{p_B}{\frac{c_A}{s_A}\left(1 - p_A\right)\left(1 - p_B\right)} \tag{A.13}$$

where we have defined,

$$\lambda \equiv v_{\text{b}} \exp\left(\epsilon\right). \tag{A.14}$$

The attractive volume of a bond λ scales exponentially with ϵ, analogous to the binding life-time ($\tau = \tau_0 \exp(\epsilon)$, Figure 2), and accordingly, is a convenient descriptor of the strength of the associations, as the static and dynamic properties of the reversibly associating polymers are extremely sensitive to the bond association energy.

The condition for the free energy minimum (eq. A.13) can be solved for the fraction p_A of associated A-stickers,

$$p_A = \frac{1}{2} \left[1 + \frac{c_B/s_B}{c_A/s_A} + \frac{1 - \sqrt{\left(1 + \left(\frac{c_A}{s_A} + \frac{c_B}{s_B}\right)\lambda\right)^2 - 4\frac{c_A}{s_A}\frac{c_B}{s_B}\lambda^2}}{\frac{c_A}{s_A}\lambda} \right] \qquad (A.15)$$

which is the degree of conversion of A stickers. It is convenient to introduce a sticker stoichiometry parameter, r, the ratio of concentrations of A and B stickers,

$$r = \frac{c_A/s_A}{c_B/s_B} = \frac{p_B}{p_A} \qquad (A.16)$$

to relate the degrees of conversion p_A to p_B:

$$p_A = \frac{p_B}{r} = \frac{1}{2} \left[1 + r^{-1} + \frac{1 - r^{-1}\sqrt{\left(r + (1+r)\frac{c_A}{s_A}\lambda\right)^2 - r\left(2\frac{c_A}{s_A}\lambda\right)^2}}{\frac{c_A}{s_A}\lambda} \right]. \qquad (A.17)$$

Substituting the condition for the free energy minimum (eq. A.13) into the free energy, we obtain the resultant minimum of the free energy density of the system:

$$\frac{F}{k_B T} = \frac{c_A}{N_A} \ln\left(c_A a^3\right) + \frac{c_B}{N_B} \ln\left(c_B a^3\right) + \frac{v}{2}(c_A + c_B)^2 + \frac{w}{6}(c_A + c_B)^3 + \chi_{AB} a^3 c_A c_B$$
$$+ \rho + \frac{c_A}{s_A} \ln\left(1 - p_A\right) + \frac{c_B}{s_B} \ln\left(1 - p_B\right) \qquad (A.18)$$

where the association strength λ enters implicitly through the fractional degrees of conversion, p_A and $p_B = r p_A$ (eqs. A.15 or A.17). The free energy is further constrained by the

relationship between p_A, p_B, and ρ: $\rho = p_A c_A / s_A = p_B c_B / s_B$ (eq. A.3). We can rewrite A.18 as

$$\frac{F}{k_{\mathrm{B}}T} = \frac{c_A}{N_A} \ln\left(c_A a^3\right) + \frac{c_B}{N_B} \ln\left(c_B a^3\right) + \frac{v}{2}(c_A + c_B)^2 + \frac{w}{6}(c_A + c_B)^3 + \chi_{AB} a^3 c_A c_B$$
$$+ \frac{c_A}{s_A}\left[p_A + \ln\left(1 - p_A\right)\right] + \frac{c_B}{s_B} \ln\left(1 - r p_A\right) \quad \text{(A.19)}$$

The phase behavior of this system of $A - B$ associative polymers can be pursued in a standard manner using thermodynamic operators obtained from the free energy density. Phase coexistence conditions can be determined by equating the exchange chemical potentials of species i in each phase required for chemical equilibrium ($\mu_i^{\mathrm{I}} = \mu_i^{\mathrm{II}}$) and the osmotic pressure in each phase needed for mechanical equilibrium ($\Pi^{\mathrm{I}} = \Pi^{\mathrm{II}}$). The chemical potentials can be calculated by differentiating the minimized free energy density, eq. A.18, with respect to the concentration of type i,

$$\frac{\mu_A}{k_{\mathrm{B}}T} = \frac{1}{k_{\mathrm{B}}T}\frac{\partial F}{\partial c_A}$$
$$= \frac{1}{N_A} + \frac{1}{N_A} \ln\left(c_A a^3\right) + v(c_A + c_B) + \frac{w}{2}(c_A + c_B)^2 + \chi_{AB} a^3 c_B + \frac{1}{s_A} \ln\left(1 - p_A\right)$$
$$\text{(A.20)}$$

$$\frac{\mu_B}{k_{\mathrm{B}}T} = \frac{1}{k_{\mathrm{B}}T}\frac{\partial F}{\partial c_B}$$
$$= \frac{1}{N_B} + \frac{1}{N_B} \ln\left(c_B a^3\right) + v(c_A + c_B) + \frac{w}{2}(c_A + c_B)^2 + \chi_{AB} a^3 c_A + \frac{1}{s_B} \ln\left(1 - r p_A\right)$$
$$\text{(A.21)}$$

These expressions correspond to the standard exchange chemical potential of a polymer–polymer–solvent mixture, with a final term appended to account for the exchange of unpaired stickers. The interaction strength, the attractive volume of a bond λ, enters the expressions for the chemical potentials through the fraction of closed stickers p_A (eqs. A.15

or A.17). Note that due to the concentration dependence of the fractional degrees of conversion, the linear term $\rho = p_A c_A / s_A = p_B c_B / s_B$ in eq. A.18 does not affect the chemical potentials (eqs. A.20-A.21).

The osmotic pressure can be calculated from the free energy density, eq. A.18, as its derivative with respect to volume at constant number of A and B molecules, or, by thermodynamic closure,

$$
\begin{aligned}
\frac{\Pi}{k_B T} &= \frac{1}{k_B T}\left(c_A \frac{\partial F}{\partial c_A} + c_B \frac{\partial F}{\partial c_B} - F \right) \\
&= \frac{c_A}{N_A} + \frac{c_B}{N_B} + \frac{v}{2}(c_A + c_B)^2 + \frac{w}{3}(c_A + c_B)^3 + \chi_{AB} a^3 c_A c_B - p_A \frac{c_A}{s_A}
\end{aligned} \tag{A.22}
$$

The first five terms are the classical virial expansion terms of a polymer mixture in solution; the final term (which is equal to $-\rho$) is attributed to the paired stickers. The sticker associations reduce the osmotic pressure by $k_B T$ per pair of bound stickers, increasing the osmotic compressibility by a term proportional to p_A / s_A, which is equal to the inverse average chain length between paired stickers. Accordingly, the zero wave-vector limit of the scattering function, as measured by X-ray or neutron scattering, will be increased with increasing sticker binding.

The spinodal condition, the stability limit of the solution, separating the unstable and metastable regions of phase space, can be calculated as

$$
\det\left(\frac{\partial^2 F}{\partial \mathbf{c}^2} \right) = \begin{vmatrix} \frac{\partial \mu_A}{\partial c_A} & \frac{\partial \mu_A}{\partial c_B} \\ \frac{\partial \mu_B}{\partial c_A} & \frac{\partial \mu_B}{\partial c_B} \end{vmatrix} = 0 \tag{A.23}
$$

with

$$
\frac{1}{k_B T} \frac{\partial \mu_A}{\partial c_A} = \frac{1}{c_A N_A} + v + w(c_A + c_B) - \frac{1}{c_A s_A}\left(\frac{r p_A^2}{r p_A^2 - 1} \right) \tag{A.24}
$$

$$
\frac{1}{k_B T} \frac{\partial \mu_B}{\partial c_B} = \frac{1}{c_B N_B} + v + w(c_A + c_B) - \frac{1}{c_B s_B}\left(\frac{r p_A^2}{r p_A^2 - 1} \right) \tag{A.25}
$$

$$\frac{1}{k_\mathrm{B}T}\frac{\partial \mu_A}{\partial c_B} = \frac{1}{k_\mathrm{B}T}\frac{\partial \mu_B}{\partial c_A} = v + w(c_A + c_B) + \chi_{AB}a^3 + \frac{1}{c_A s_B}\left(\frac{rp_A}{rp_A^2 - 1}\right). \tag{A.26}$$

These binodal and spinodal conditions are used to calculate the phase boundaries in the phase diagrams of Figures 9-10, as well as corresponding discussion in Section 5 of asymptotic behavior and physics in different regimes.

References

(1) Creton, C. 50th Anniversary Perspective: Networks and Gels: Soft but Dynamic and Tough. *Macromolecules* **2017**, *50*, 8297–8316, DOI: `10.1021/acs.macromol.7b01698`.

(2) Gu, Y. W.; Zhao, J. L.; Johnson, J. A. Polymer Networks: From Plastics and Gels to Porous Frameworks. *Angew. Chem., Int. Ed.* **2020**, 5022–5049, DOI: `10.1002/anie.201902900`.

(3) Danielsen, S. P. O. et al. Molecular Characterization of Polymer Networks. *Chem. Rev.* **2021**, *121*, 5042–5092, DOI: `10.1021/acs.chemrev.0c01304`.

(4) Cordier, P.; Tournilhac, F.; Soulie-Ziakovic, C.; Leibler, L. Self-Healing and Thermoreversible Rubber from Supramolecular Assembly. *Nature* **2008**, *451*, 977–980, DOI: `10.1038/nature06669`.

(5) Syrett, J. A.; Becer, C. R.; Haddleton, D. M. Self-Healing and Self-Mendable Polymers. *Polym. Chem.* **2010**, *1*, 978–987, DOI: `10.1039/c0py00104j`.

(6) Stukalin, E. B.; Cai, L. H.; Kumar, N. A.; Leibler, L.; Rubinstein, M. Self-Healing of Unentangled Polymer Networks with Reversible Bonds. *Macromolecules* **2013**, *46*, 7525–7541, DOI: `10.1021/ma401111n`.

(7) Campanella, A.; Dohler, D.; Binder, W. H. Self-Healing in Supramolecular Polymers. *Macromol. Rapid Commun.* **2018**, *39*, 1700739, DOI: `10.1002/marc.201700739`.

(8) Wojtecki, R. J.; Meador, M. A.; Rowan, S. J. Using the Dynamic Bond to Access Macroscopically Responsive Structurally Dynamic Polymers. *Nat. Mater.* **2011**, *10*, 14–27, DOI: `10.1038/Nmat2891`.

(9) Stuart, M. A. C.; Huck, W. T. S.; Genzer, J.; Muller, M.; Ober, C.; Stamm, M.; Sukhorukov, G. B.; Szleifer, I.; Tsukruk, V. V.; Urban, M.; Winnik, F.; Zauscher, S.;

Luzinov, I.; Minko, S. Emerging Applications of Stimuli-Responsive Polymer Materials. *Nat. Mater.* **2010**, *9*, 101–113, DOI: `10.1038/Nmat2614`.

(10) Annable, T.; Buscall, R.; Ettelaie, R.; Whittlestone, D. The Rheology of Solutions of Associating Polymers—Comparison of Experimental Behavior with Transient Network Theory. *J. Rheol.* **1993**, *37*, 695–726, DOI: `10.1122/1.550391`.

(11) Bates, F. S.; Hillmyer, M. A.; Lodge, T. P.; Bates, C. M.; Delaney, K. T.; Fredrickson, G. H. Multiblock Polymers: Panacea or Pandora's Box? *Science* **2012**, *336*, 434–440, DOI: `10.1126/science.1215368`.

(12) Bates, C. M.; Bates, F. S. 50th Anniversary Perspective: Block Polymers-Pure Potential. *Macromolecules* **2017**, *50*, 3–22, DOI: `10.1021/acs.macromol.6b02355`.

(13) Li, P. L.; Banjade, S.; Cheng, H. C.; Kim, S.; Chen, B.; Guo, L.; Llaguno, M.; Hollingsworth, J. V.; King, D. S.; Banani, S. F.; Russo, P. S.; Jiang, Q. X.; Nixon, B. T.; Rosen, M. K. Phase Transitions in the Assembly of Multivalent Signalling Proteins. *Nature* **2012**, *483*, 336–U129, DOI: `10.1038/nature10879`.

(14) Feric, M.; Vaidya, N.; Harmon, T. S.; Mitrea, D. M.; Zhu, L.; Richardson, T. M.; Kriwacki, R. W.; Pappu, R. V.; Brangwynne, C. P. Coexisting Liquid Phases Underlie Nucleolar Subcompartments. *Cell* **2016**, *165*, 1686–1697, DOI: `10.1016/j.cell.2016.04.047`.

(15) Boeynaems, S.; Holehouse, A. S.; Weinhardt, V.; Kovacs, D.; Van Lindt, J.; Larabell, C.; Van Den Bosch, L.; Das, R.; Tompa, P. S.; Pappu, R. V.; Gitler, A. D. Spontaneous Driving Forces Give Rise to Protein-RNA Condensates with Coexisting Phases and Complex Material Properties. *Proc. Natl. Acad. Sci. U.S.A.* **2019**, *116*, 7889–7898, DOI: `10.1073/pnas.1821038116`.

(16) Hildebrand, E. M.; Dekker, J. Mechanisms and Functions of Chromo-

some Compartmentalization. *Trends Biochem. Sci.* **2020**, *45*, 385–396, DOI: `10.1016/j.tibs.2020.01.002`.

(17) Brackley, C. A.; Marenduzzo, D. Bridging-Induced Microphase Separation: Photobleaching Experiments, Chromatin Domains and the Need for Active Reactions. *Brief. Funct. Genomics* **2020**, *19*, 111–118, DOI: `10.1093/bfgp/elz032`.

(18) Hilbert, L.; Sato, Y.; Kuznetsova, K.; Bianucci, T.; Kimura, H.; Julicher, F.; Honigmann, A.; Zaburdaev, V.; Vastenhouw, N. L. Transcription Organizes Euchromatin via Microphase Separation. *Nat. Commun.* **2021**, *12*, 1360, DOI: `10.1038/s41467-021-21589-3`.

(19) Zhang, Y. J.; Xu, B.; Weiner, B. G.; Meir, Y.; Wingreen, N. S. Decoding the Physical Principles of Two-Component Biomolecular Phase Separation. *eLife* **2021**, *10*, e62403, DOI: `10.7554/eLife.62403`.

(20) Laghmach, R.; Alshareedah, I.; Pham, M.; Raju, M.; Banerjee, P. R.; Potoyan, D. A. RNA Chain Length and Stoichiometry Govern Surface Tension and Stability of Protein–RNA Condensates. *iScience* **2022**, *25*, 104105, DOI: `10.1016/j.isci.2022.104105`.

(21) Lairez, D.; Adam, M.; Carton, J. P.; Raspaud, E. Aggregation of Telechelic Triblock Copolymers: From Animals to Flowers. *Macromolecules* **1997**, *30*, 6798–6809, DOI: `10.1021/ma970666m`.

(22) Chen, J. F.; Garcia, E. S.; Zimmerman, S. C. Intramolecularly Cross-Linked Polymers: From Structure to Function with Applications as Artificial Antibodies and Artificial Enzymes. *Acc. Chem. Res.* **2020**, *53*, 1244–1256, DOI: `10.1021/acs.accounts.0c00178`.

(23) Formanek, M.; Rovigatti, L.; Zaccarelli, E.; Sciortino, F.; Moreno, A. J. Gel Formation

in Reversibly Cross-Linking Polymers. *Macromolecules* **2021**, *54*, 6613–6627, DOI: `10.1021/acs.macromol.0c02670`.

(24) Pomposo, J. A.; Rubio-Cervilla, J.; Moreno, A. J.; Lo Verso, F.; Bacova, P.; Arbe, A.; Colmenero, J. Folding Single Chains to Single-Chain Nanoparticles via Reversible Interactions: What Size Reduction Can One Expect? *Macromolecules* **2017**, *50*, 1732–1739, DOI: `10.1021/acs.macromol.6b02427`.

(25) Sing, C. E.; Alexander-Katz, A. Equilibrium Structure and Dynamics of Self-Associating Single Polymers. *Macromolecules* **2011**, *44*, 6962–6971, DOI: `10.1021/ma200830t`.

(26) Sing, C. E.; Alexander-Katz, A. Designed Molecular Mechanics Using Self-Associating Polymers. *Soft Matter* **2012**, *8*, 11871–11879, DOI: `10.1039/c2sm26276b`.

(27) Chen, Q.; Tudryn, G. J.; Colby, R. H. Ionomer Dynamics and the Sticky Rouse Model. *J. Rheol.* **2013**, *57*, 1441–1462, DOI: `10.1122/1.4818868`.

(28) Chen, Q.; Huang, C. W.; Weiss, R. A.; Colby, R. H. Viscoelasticity of Reversible Gelation for Ionomers. *Macromolecules* **2015**, *48*, 1221–1230, DOI: `10.1021/ma502280g`.

(29) Hall, L. M.; Seitz, M. E.; Winey, K. I.; Opper, K. L.; Wagener, K. B.; Stevens, M. J.; Frischknecht, A. L. Ionic Aggregate Structure in Ionomer Melts: Effect of Molecular Architecture on Aggregates and the Ionomer Peak. *J. Am. Chem. Soc.* **2012**, *134*, 574–587, DOI: `10.1021/ja209142b`.

(30) Mordvinkin, A.; Suckow, M.; Böhme, F.; Colby, R. H.; Creton, C.; Saalwächter, K. Hierarchical Sticker and Sticky Chain Dynamics in Self-Healing Butyl Rubber Ionomers. *Macromolecules* **2019**, *52*, 4169–4184, DOI: `10.1021/acs.macromol.9b00159`.

(31) Leibler, L.; Rubinstein, M.; Colby, R. H. Dynamics of Reversible Networks. *Macromolecules* **1991**, *24*, 4701–4707, DOI: `10.1021/ma00016a034`.

(32) Semenov, A. N.; Rubinstein, M. Thermoreversible Gelation in Solutions of Associative Polymers. 1. Statics. *Macromolecules* **1998**, *31*, 1373–1385, DOI: `10.1021/ma970616h`.

(33) Rubinstein, M.; Semenov, A. N. Thermoreversible Gelation in Solutions of Associating Polymers. 2. Linear Dynamics. *Macromolecules* **1998**, *31*, 1386–1397, DOI: `10.1021/ma970617+`.

(34) Rubinstein, M.; Semenov, A. N. Dynamics of Entangled Solutions of Associating Polymers. *Macromolecules* **2001**, *34*, 1058–1068, DOI: `10.1021/ma0013049`.

(35) Semenov, A. N.; Rubinstein, M. Dynamics of Entangled Associating Polymers with Large Aggregates. *Macromolecules* **2002**, *35*, 4821–4837, DOI: `10.1021/ma0117965`.

(36) Tanaka, F. Theory of Thermoreversible Gelation. *Macromolecules* **1989**, *22*, 1988–1994, DOI: `10.1021/ma00194a077`.

(37) Tanaka, F. Thermodynamic Theory of Network-Forming Polymer-Solutions. *Macromolecules* **1990**, *23*, 3784–3789, DOI: `10.1021/ma00218a012`.

(38) Tanaka, F. Thermodynamic Theory of Network-Forming Polymer-Solutions .2. Equilibrium Gelation by Conterminous Cross-Linking. *Macromolecules* **1990**, *23*, 3790–3795, DOI: `10.1021/ma00218a013`.

(39) Tanaka, F.; Stockmayer, W. H. Thermoreversible Gelation with Junctions of Variable Multiplicity. *Macromolecules* **1994**, *27*, 3943–3954, DOI: `10.1021/ma00092a039`.

(40) Ishida, M.; Tanaka, F. Theoretical Study of the Postgel Regime in Thermoreversible Gelation. *Macromolecules* **1997**, *30,* 3900–3909, DOI: `10.1021/ma960580d`.

(41) Stockmayer, W. H. Theory of molecular size distribution and gel formation in branched-chain polymers. *J. Chem. Phys.* **1943**, *11*, 45–55, DOI: `10.1063/1.1723803`.

(42) Stockmayer, W. H. Theory of Molecular Size Distribution and Gel Formation in Branched Polymers II General Crosslinking. *J. Chem. Phys.* **1944**, *12*, 125–131, DOI: `10.1063/1.1723922`.

(43) Stockmayer, W. H. Thermoreversible Gelation via Multichain Junctions. *Macromolecules* **1991**, *24*, 6367–6368, DOI: `10.1021/ma00023a052`.

(44) Flory, P. J. Molecular size distribution in three dimensional polymers. I. Gelation. *J. Am. Chem. Soc.* **1941**, *63*, 3083–3090, DOI: `10.1021/ja01856a061`.

(45) Feldman, K. E.; Kade, M. J.; Meijer, E. W.; Hawker, C. J.; Kramer, E. J. Phase Behavior of Complementary Multiply Hydrogen Bonded End-Functional Polymer Blends. *Macromolecules* **2010**, *43*, 5121–5127, DOI: `10.1021/ma1003776`.

(46) Simon, M.; Prause, A.; Zauscher, S.; Gradzielski, M. Self-Assembled Single-Stranded DNA Nano-Networks in Solution and at Surfaces. *Biomacromolecules* **2022**, *23*, 1242–1250, DOI: `10.1021/acs.biomac.1c01493`.

(47) Fu, J.; Fares, H. M.; Schlenoff, J. B. Ion-Pairing Strength in Polyelectrolyte Complexes. *Macromolecules* **2017**, *50*, 1066–1074, DOI: `10.1021/acs.macromol.6b02445`.

(48) Lalwani, S. M.; Eneh, C. I.; Lutkenhaus, J. L. Emerging Trends in the Dynamics of Polyelectrolyte Complexes. *Phys. Chem. Chem. Phys.* **2020**, *22*, 24157–24177, DOI: `10.1039/d0cp03696j`.

(49) Filippidi, E.; Cristiani, T. R.; Eisenbach, C. D.; Waite, J. H.; Israelachvili, J. N.; Ahn, B. K.; Valentine, M. T. Toughening Elastomers using Mussel-Inspired Iron–Catechol Complexes. *Science* **2017**, *358*, 502–505, DOI: `10.1126/science.aao0350`.

(50) Brassinne, J.; Cadix, A.; Wilson, J.; van Ruymbeke, E. Dissociating Sticker Dynamics

from Chain Relaxation in Supramolecular Polymer Networks—The Importance of Free Partner! *J. Rheol.* **2017**, *61*, 1123–1134, DOI: `10.1122/1.4997594`.

(51) Holten-Andersen, N.; Harrington, M. J.; Birkedal, H.; Lee, B. P.; Messersmith, P. B.; Lee, K. Y. C.; Waite, J. H. pH-Induced Metal-Ligand Cross-Links Inspired by Mussel Yield Self-Healing Polymer Networks with Near-Covalent Elastic Moduli. *Proc. Natl. Acad. Sci. U.S.A.* **2011**, *108*, 2651–2655, DOI: `10.1073/pnas.1015862108`.

(52) Schauser, N. S.; Sanoja, G. E.; Bartels, J. M.; Jain, S. K.; Hu, J. G.; Han, S. I.; Walker, L. M.; Helgeson, M. E.; Seshadri, R.; Segalman, R. A. Decoupling Bulk Mechanics and Mono- and Multivalent Ion Transport in Polymers Based on Metal–Ligand Coordination. *Chem. Mater.* **2018**, *30*, 5759–5769, DOI: `10.1021/acs.chemmater.8b02633`.

(53) Mareliati, M.; Tadiello, L.; Guerra, S.; Giannini, L.; Schrettl, S.; Weder, C. Metal–Ligand Complexes as Dynamic Sacrificial Bonds in Elastic Polymers. *Macromolecules* **2022**, *55*, 5164–5175, DOI: `10.1021/acs.macromol.2c00752`.

(54) Guo, X. H.; Abdala, A. A.; May, B. L.; Lincoln, S. F.; Khan, S. A.; Prud'homme, R. K. Novel Associative Polymer Networks Based on Cyclodextrin Inclusion Compounds. *Macromolecules* **2005**, *38*, 3037–3040, DOI: `10.1021/ma050071o`.

(55) Li, L.; Guo, X. H.; Wang, J.; Liu, P.; Prud'homme, R. K.; May, B. L.; Lincoln, S. F. Polymer Networks Assembled by Host–Guest Inclusion between Adamantyl and β-Cyclodextrin Substituents on Poly(acrylic acid) in Aqueous Solution. *Macromolecules* **2008**, *41*, 8677–8681, DOI: `10.1021/ma8020147`.

(56) Zhang, C. R.; Cai, Y. M.; Zhao, Q. Coacervation between Two Positively Charged Poly(ionic liquid)s. *Macromol. Rapid Commun.* **2022**, *43*, 2200191, DOI: `10.1002/marc.202200191`.

(57) Vidal, F.; Gomezcoello, J.; Lalancette, R. A.; Jakle, F. Lewis Pairs as Highly Tunable Dynamic Cross-Links in Transient Polymer Networks. *J. Am. Chem. Soc.* **2019**, *141*, 15963–15971, DOI: `10.1021/jacs.9b07452`.

(58) Zhang, Z. J.; Chen, Q.; Colby, R. H. Dynamics of Associative Polymers. *Soft Matter* **2018**, *14*, 2961–2977, DOI: `10.1039/c8sm00044a`.

(59) Wu, S. L.; Chen, Q. Advances and New Opportunities in the Rheology of Physically and Chemically Reversible Polymers. *Macromolecules* **2022**, *55*, 697–714, DOI: `10.1021/acs.macromol.1c01605`.

(60) Cai, P. C.; Su, B.; Zou, L.; Webber, M. J.; Heilshorn, S. C.; Spakowitz, A. J. Rheological Characterization and Theoretical Modeling Establish Molecular Design Rules for Tailored Dynamically Associating Polymers. *ACS Cent. Sci.* **2022**, *8*, 1318–1327, DOI: `10.1021/acscentsci.2c00432`.

(61) Painter, P. C.; Graf, J.; Coleman, M. M. A Lattice Model Describing Hydrogen-Bonding in Polymer Mixtures. *J. Chem. Phys.* **1990**, *92*, 6166–6174, DOI: `10.1063/1.458340`.

(62) Painter, P. C.; Park, Y.; Coleman, M. M. Thermodynamics of Hydrogen-Bonding in Polymer Blends .1. Application of Association Models. *Macromolecules* **1989**, *22*, 570–579, DOI: `10.1021/ma00192a011`.

(63) Painter, P. C.; Park, Y.; Coleman, M. M. Hydrogen-Bonding in Polymer Blends .2. Theory. *Macromolecules* **1988**, *21*, 66–72, DOI: `10.1021/ma00179a015`.

(64) Painter, P. C.; Graf, J.; Coleman, M. M. A Lattice Model Describing Hydrogen-Bonding in Polymer Mixtures. *J. Chem. Phys.* **1990**, *92*, 6166–6174, DOI: `10.1063/1.458340`.

(65) Tanaka, F.; Ishida, M. Microphase Formation in Mixtures of Associating Polymers. *Macromolecules* **1997**, *30*, 1836–1844, DOI: `10.1021/ma961457p`.

(66) Tanaka, F.; Ishida, N. Thermoreversible Gelation with Two-Component Networks. *Macromolecules* **1999**, *32*, 1271–1283, DOI: `10.1021/ma981279v`.

(67) Tanaka, F. Thermoreversible Gelation with Two-Component Mixed Cross-Link Junctions of Variable Multiplicity in Ternary Polymer Solutions. *Gels* **2021**, *7*, 89, DOI: `10.3390/gels7030089`.

(68) Angerman, H. J.; ten Brinke, G. Weak Segregation Theory of Microphase Separation in Associating Binary Homopolymer Blends. *Macromolecules* **1999**, *32*, 6813–6820, DOI: `10.1021/ma981518e`.

(69) Hoy, R. S.; Fredrickson, G. H. Thermoreversible Associating Polymer Networks. I. Interplay of Thermodynamics, Chemical Kinetics, and Polymer Physics. *J. Chem. Phys.* **2009**, *131*, 224902, DOI: `10.1063/1.3268777`.

(70) Mohan, A.; Elliot, R.; Fredrickson, G. H. Field-Theoretic Model of Inhomogeneous Supramolecular Polymer Networks and Gels. *J. Chem. Phys.* **2010**, *133*, 174903, DOI: `10.1063/1.3497038`.

(71) Mester, Z.; Mohan, A.; Fredrickson, G. H. Macro- and Microphase Separation in Multifunctional Supramolecular Polymer Networks. *Macromolecules* **2011**, *44*, 9411–9423, DOI: `10.1021/ma201551c`.

(72) Fredrickson, G. H.; Delaney, K. T. Coherent States Field Theory in Supramolecular Polymer Physics. *J. Chem. Phys.* **2018**, *148*, 204904, DOI: `10.1063/1.5027582`.

(73) Loverde, S. M.; Ermoshkin, A. V.; de la Cruz, M. O. Thermodynamics of Reversibly Associating Ideal Chains. *J. Polym. Sci., Part B: Polym. Phys.* **2005**, *43*, 796–804, DOI: `10.1002/polb.20372`.

(74) Prusty, D.; Pryamitsyn, V.; de la Cruz, M. O. Thermodynamics of Associative Polymer Blends. *Macromolecules* **2018**, *51*, 5918–5932, DOI: `10.1021/acs.macromol.8b00661`.

(75) Choi, J. M.; Hyman, A. A.; Pappu, R. V. Generalized Models for Bond Percolation Transitions of Associative Polymers. *Phys. Rev. E* **2020**, *102*, DOI: `10.1103/PhysRevE.102.042403`.

(76) Zaldivar, G.; Tagliazucchi, M. Layer-by-Layer Self-Assembly of Polymers with Pairing Interactions. *ACS Macro Lett.* **2016**, *5*, 862–866, DOI: `10.1021/acsmacrolett.6b00258`.

(77) Sing, C. E.; Perry, S. L. Recent Progress in the Science of Complex Coacervation. *Soft Matter* **2020**, *16*, 2885–2914, DOI: `10.1039/D0SM00001A`.

(78) Perry, S. L.; Sing, C. E. PRISM-Based Theory of Complex Coacervation: Excluded Volume versus Chain Correlation. *Macromolecules* **2015**, *48*, 5040–5053, DOI: `10.1021/acs.macromol.5b01027`.

(79) Lytle, T. K.; Sing, C. E. Transfer Matrix Theory of Polymer Complex Coacervation. *Soft Matter* **2017**, *13*, 7001–7012, DOI: `10.1039/c7sm01080j`.

(80) Salehi, A.; Larson, R. G. A Molecular Thermodynamic Model of Complexation in Mixtures of Oppositely Charged Polyelectrolytes with Explicit Account of Charge Association/Dissociation. *Macromolecules* **2016**, *49*, 9706–9719, DOI: `10.1021/acs.macromol.6b01464`.

(81) Friedowitz, S.; Salehi, A.; Larson, R. G.; Qin, J. Role of Electrostatic Correlations in Polyelectrolyte Charge Association. *J. Chem. Phys.* **2018**, *149*, 163335, DOI: `10.1063/1.5034454`.

(82) Delaney, K. T.; Fredrickson, G. H. Theory of Polyelectrolyte Complexation-Complex Coacervates Are Self-Coacervates. *J. Chem. Phys.* **2017**, *146*, 224902, DOI: `10.1063/1.4985568`.

(83) Danielsen, S. P. O.; McCarty, J.; Shea, J.-E.; Delaney, K. T.; Fredrickson, G. H. Molecular Design of Self-Coacervation Phenomena in Block Polyampholytes. *Proc. Natl. Acad. Sci. U. S. A.* **2019**, *116*, 8224–8232, DOI: `10.1073/pnas.1900435116`.

(84) Danielsen, S. P. O.; McCarty, J.; Shea, J.-E.; Delaney, K. T.; Fredrickson, G. H. Small Ion Effects on Self-Coacervation Phenomena in Block Polyampholytes. *J. Chem. Phys.* **2019**, *151*, 034904, DOI: `10.1063/1.5109045`.

(85) Rubinstein, M.; Liao, Q.; Panyukov, S. Structure of Liquid Coacervates Formed by Oppositely Charged Polyelectrolytes. *Macromolecules* **2018**, *51*, 9572–9588, DOI: `10.1021/acs.macromol.8b02059`.

(86) Danielsen, S. P. O.; Panyukov, S.; Rubinstein, M. Ion Pairing and the Structure of Gel Coacervates. *Macromolecules* **2020**, *53*, 9420–9442, DOI: `10.1021/acs.macromol.0c01360`.

(87) Debais, G.; Tagliazucchi, M. Two Sides of the Same Coin: A Unified Theoretical Treatment of Polyelectrolyte Complexation in Solution and Layer-by-Layer Films. *Macromolecules* **2022**, *55*, 5263–5275, DOI: `10.1021/acs.macromol.2c002505263`.

(88) Espinosa, J. R.; Joseph, J. A.; Sanchez-Burgos, I.; Garaizar, A.; Frenkel, D.; Collepardo-Guevara, R. Liquid Network Connectivity Regulates the Stability and Composition of Biomolecular Condensates with Many Components. *Proc. Natl. Acad. Sci. U.S.A.* **2020**, *117*, 13238–13247, DOI: `10.1073/pnas.1917569117`.

(89) Martin, E. W.; Holehouse, A. S.; Peran, I.; Farag, M.; Incicco, J. J.; Bremer, A.; Grace, C. R.; Soranno, A.; Pappu, R. V.; Mittag, T. Valence and Patterning of Aro-

matic Residues Determine the Phase Behavior of Prion-like Domains. *Science* **2020**, *367*, 694–699, DOI: `10.1126/science.aaw8653`.

(90) Ranganathan, S.; Shakhnovich, E. I. Dynamic Metastable Long-Living Droplets Formed by Sticker–Spacer Proteins. *eLife* **2020**, *9*, e56159, DOI: `10.7554/eLife.56159`.

(91) Rubinstein, M.; Colby, R. H. *Polymer Physics*; Oxford University Press: New York, 2003.

(92) Lodge, T. P.; Hiemenz, P. C. *Polymer Chemistry*; CRC Press, Taylor & Francis Group: Boca Raton, 2020.

(93) Scott, R. L. The Thermodynamics of High Polymer Solutions .V. Phase Equilibria in the Ternary System - Polymer-1 Polymer-2 Solvent. *J. Chem. Phys.* **1949**, *17*, 279–284, DOI: `10.1063/1.1747239`.

(94) Hsu, C. C.; Prausnitz, J. M. Thermodynamics of Polymer Compatibility in Ternary-Systems. *Macromolecules* **1974**, *7*, 320–324, DOI: `10.1021/ma60039a012`.

(95) Khokhlov, A. R. Concept of Quasimonomers and Its Application to Some Problems of Polymer Statistics. *Polymer* **1978**, *19*, 1387–1396, DOI: `10.1016/0032-3861(78)90090-3`.

(96) Schaefer, D. W.; Joanny, J. F.; Pincus, P. Dynamics of Semiflexible Polymers in Solution. *Macromolecules* **1980**, *13*, 1280–1289, DOI: `10.1021/ma60077a048`.

(97) de Gennes, P. G. Effect of Cross-Links on a Mixture of Polymers. *J. Phys., Lett.* **1979**, *40*, L69–L72.

(98) Shibayama, M.; Ikkai, F.; Nomura, S. Microscopic Structure and Viscosity Behaviors of Ion-Complexed Polymer Gels. *Macromol. Symp.* **1995**, *93*, 277–281, DOI: `10.1002/masy.19950930133`.

(99) Shibayama, M.; Ikkai, F.; Moriwaki, R.; Nomura, S. Complexation of Poly(Vinyl Alcohol)–Congo Red Aqueous Solutions .1. Viscosity Behavior and Gelation Mechanism. *Macromolecules* **1994**, *27*, 1738–1743, DOI: `10.1021/ma00085a011`.

(100) Flory, P. J. Molecular Size Distribution in Linear Condensation Polymers. *J. Am. Chem. Soc.* **1936**, *58*, 1877–1885, DOI: `10.1021/ja01301a016`.

(101) Stockmayer, W. H. Molecular Distribution in Condensation Polymers. *J. Polym. Sci.* **1952**, *9*, 69–71, DOI: `10.1002/pol.1952.120090106`.

(102) Gordon, M. Goods Theory of Cascade Processes Applied to Statistics of Polymer Distributions. *Proc. R. Soc. London, Ser. A* **1962**, *268*, 240–256, DOI: `10.1098/rspa.1962.0136`.

(103) Miller, D. R.; Macosko, C. W. New Derivation of Post Gel Properties of Network Polymers. *Macromolecules* **1976**, *9*, 206–211, DOI: `10.1021/ma60050a004`.

(104) Macosko, C. W.; Miller, D. R. New Derivation of Average Molecular-Weights of Nonlinear Polymers. *Macromolecules* **1976**, *9*, 199–206, DOI: `10.1021/ma60050a003`.

(105) Gillmor, J. R.; Connelly, R. W.; Colby, R. H.; Tan, J. S. Effect of Sodium Poly(Styrene Sulfonate) on Thermoreversible Gelation of Gelatin. *J. Polym. Sci., Part B: Polym. Phys.* **1999**, *37*, 2287–2295, DOI: `10.1002/(Sici)1099-0488(19990815)37:16<2287::Aid-Polb31>3.3.Co;2-E`.

(106) Bowman, W. A.; Rubinstein, M.; Tan, J. S. Polyelectrolyte–Gelatin Complexation: Light-Scattering Study. *Macromolecules* **1997**, *30*, 3262–3270, DOI: `10.1021/ma961915u`.

(107) Potier, M.; Tea, L.; Benyahia, L.; Nicolai, T.; Renou, F. Viscosity of Aqueous Polysaccharide Solutions and Selected Homogeneous Binary Mixtures. *Macromolecules* **2020**, *53*, 10514–10525, DOI: `10.1021/acs.macromol.0c02157`.

(108) Wang, J.; Li, L.; Guo, X. H.; Zheng, L.; Pham, D. T.; Lincoln, S. F.; Ngo, H. T.; Clements, P.; May, B. L.; Prud'homme, R. K.; Easton, C. J. Aggregation of Hydrophobic Substituents of Poly(acrylate)s and Their Competitive Complexation by β- and γ-Cyclodextrins and Their Linked Dimers in Aqueous Solution. *Ind. Eng. Chem. Res.* **2011**, *50*, 7566–7571, DOI: 10.1021/ie101705e.

(109) Wintgens, V.; Daoud-Mahammed, S.; Gref, R.; Bouteiller, L.; Amiel, C. Aqueous Polysaccharide Associations Mediated by β-Cyclodextrin Polymers. *Biomacromolecules* **2008**, *9*, 1434–1442, DOI: 10.1021/bm800019g.

(110) de Kruif, C. G.; Weinbreck, F.; de Vries, R. Complex Coacervation of Proteins and Anionic Polysaccharides. *Curr. Opin. Colloid Interface Sci.* **2004**, *9*, 340–349, DOI: 10.1016/j.cocis.2004.09.006.

(111) van der Gucht, J.; Spruijt, E.; Lemmers, M.; Cohen Stuart, M. A. Polyelectrolyte Complexes: Bulk Phases and Colloidal Systems. *J. Colloid Interface Sci.* **2011**, *361*, 407–22, DOI: 10.1016/j.jcis.2011.05.080.

(112) Hoffman, A. S. Hydrogels for Biomedical Applications. *Adv. Drug Deliv. Rev.* **2002**, *54*, 3–12, DOI: 10.1016/S0169-409x(01)00239-3.

(113) Li, X. Y.; Fang, Y. P.; Al-Assaf, S.; Phillips, G. O.; Yao, X. L.; Zhang, Y. F.; Zhao, M.; Zhang, K.; Jiang, F. T. Complexation of Bovine Serum Albumin and Sugar Beet Pectin: Structural Transitions and Phase Diagram. *Langmuir* **2012**, *28*, 10164–10176, DOI: 10.1021/la302063u.

(114) Doublier, J. L.; Garnier, C.; Renard, D.; Sanchez, C. Protein–Polysaccharide Interactions. *Curr. Opin. Colloid Interface Sci.* **2000**, *5*, 202–214, DOI: 10.1016/S1359-0294(00)00054-6.

(115) Kaibara, K.; Okazaki, T.; Bohidar, H. B.; Dubin, P. L. pH-Induced Coacervation

in Complexes of Bovine Serum Albumin and Cationic Polyelectrolytes. *Biomacromolecules* **2000**, *1*, 100–107, DOI: `10.1021/bm990006k`.

(116) Perry, S. L. Phase Separation: Bridging Polymer Physics and Biology. *Curr. Opin. Colloid Interface Sci.* **2019**, *39*, 86–97, DOI: `10.1016/j.cocis.2019.01.007`.

(117) Schuster, B. S.; Regy, R. M.; Dolan, E. M.; Ranganath, A. K.; Jovic, N.; Khare, S. D.; Shi, Z.; Mittal, J. Biomolecular Condensates: Sequence Determinants of Phase Separation, Microstructural Organization, Enzymatic Activity, and Material Properties. *J. Phys. Chem. B* **2021**, *125*, 3441–3451, DOI: `10.1021/acs.jpcb.0c11606`.

(118) Bhandari, K.; Cotten, M. A.; Kim, J.; Rosen, M. K.; Schmit, J. D. Structure–Function Properties in Disordered Condensates. *J. Phys. Chem. B* **2021**, *125*, 467–476, DOI: `10.1021/acs.jpcb.0c11057`.

(119) Norioka, C.; Okita, K.; Mukada, M.; Kawamura, A.; Miyata, T. Biomolecularly Stimuli-Responsive Tetra-Poly(ethylene glycol) that Undergoes Sol–Gel Transition in Response to a Target Biomolecule. *Polym. Chem.* **2017**, *8*, 6378–6385, DOI: `10.1039/c7py01370a`.

(120) Suh, J. M.; Bae, S. J.; Jeong, B. Thermogelling Multiblock Poloxamer Aqueous Solutions with Closed-Loop Sol–Gel–Sol Transitions upon Increasing pH. *Adv. Mater.* **2005**, *17*, 118–120, DOI: `10.1002/adma.200400905`.

(121) Ishikawa, S.; Iwanaga, Y.; Uneyama, T.; Li, X.; Hojo, H.; Fujinaga, I.; Katashima, T.; Saito, T.; Chung, U.; Sakumichi, N.; Sakai, T. 2022, DOI: `10.48550/arXiv.2202.09754`.

(122) Feng, Y.; Weiss, R. A.; Han, C. C. Compatibilization of Polymer Blends by Complexation .3. Structure Pinning During Phase Separation of Ionomer/Polyamide Blends. *Macromolecules* **1996**, *29*, 3925–3930, DOI: `10.1021/ma952016t`.

(123) Tucker, R. T.; Han, C. C.; Dobrynin, A. V.; Weiss, R. A. Small-Angle Neutron Scattering Analysis of Blends with Very Strong Intermolecular Interactions: Polyamide/Ionomer Blends. *Macromolecules* **2003**, *36*, 4404–4410, DOI: `10.1021/ma0341972`.

(124) Spruijt, E.; Westphal, A. H.; Borst, J. W.; Stuart, M. A. C.; van der Gucht, J. Binodal Compositions of Polyeleetrolyte Complexes. *Macromolecules* **2010**, *43*, 6476–6484, DOI: `10.1021/ma101031t`.

(125) Li, L.; Srivastava, S.; Andreev, M.; Marciel, A. B.; de Pablo, J. J.; Tirrell, M. V. Phase Behavior and Salt Partitioning in Polyelectrolyte Complex Coacervates. *Macromolecules* **2018**, *51*, 2988–2995, DOI: `10.1021/acs.macromol.8b00238`.

(126) Zhang, P. F.; Shen, K.; Alsaifi, N. M.; Wang, Z. G. Salt Partitioning in Complex Coacervation of Symmetric Polyelectrolytes. *Macromolecules* **2018**, *51*, 5586–5593, DOI: `10.1021/acs.macromol.8b00726`.

(127) Zhang, P. F.; Alsaifi, N. M.; Wu, J. Z.; Wang, Z. G. Polyelectrolyte Complex Coacervation: Effects of Concentration Asymmetry. *J. Chem. Phys.* **2018**, *149*, 163303, DOI: `10.1063/1.5028524`.

(128) Zhang, R.; Shklovskii, B. T. Phase Diagram of Solution of Oppositely Charged Polyelectrolytes. *Phys. A* **2005**, *352*, 216–238, DOI: `10.1016/j.physa.2004.12.037`.

(129) Castelnovo, M.; Joanny, J. F. Phase Diagram of Diblock Polyampholyte Solutions. *Macromolecules* **2002**, *35*, 4531–4538, DOI: `10.1021/ma012097v`.

(130) Shusharina, N. P.; Zhulina, E. B.; Dobrynin, A. V.; Rubinstein, M. Scaling Theory of Diblock Polyampholyte Solutions. *Macromolecules* **2005**, *38*, 8870–8881, DOI: `10.1021/ma051324g`.

(131) Borue, V. Y.; Erukhimovich, I. Y. A Statistical-Theory of Globular Polyelectrolyte Complexes. *Macromolecules* **1990**, *23*, 3625–3632, DOI: `10.1021/ma00217a015`.

(132) Wang, Z. W.; Rubinstein, M. Regimes of Conformational Transitions of a Diblock Polyampholyte. *Macromolecules* **2006**, *39*, 5897–5912, DOI: `10.1021/ma0607517`.

(133) Yan, V. T.; Narayanan, A.; Wiegantr, T.; Julicher, F.; Grill, S. W. A Condensate Dynamic Instability Orchestrates Actomyosin Cortex Activation. *Nature* **2022**, *609*, DOI: `10.1038/s41586-022-05084-3`.

(134) Aponte-Rivera, C.; Rubinstein, M. Dynamic Coupling in Unentangled Liquid Coacervates Formed by Oppositely Charged Polyelectrolytes. *Macromolecules* **2021**, *54*, 1783–1800, DOI: `10.1021/acs.macromol.0c01393`.

(135) Yount, W. C.; Loveless, D. M.; Craig, S. L. Small-Molecule Dynamics and Mechanisms Underlying the Macroscopic Mechanical Properties of Coordinatively Cross-Linked Polymer Networks. *J. Am. Chem. Soc.* **2005**, *127*, 14488–14496, DOI: `10.1021/ja054298a`.

(136) Loveless, D. M.; Jeon, S. L.; Craig, S. L. Rational Control of Viscoelastic Properties in Multicomponent Associative Polymer Networks. *Macromolecules* **2005**, *38*, 10171–10177, DOI: `10.1021/ma0518611`.

(137) Schauser, N. S.; Seshadri, R.; Segalman, R. A. Multivalent Ion Conduction in Solid Polymer Systems. *Mol. Syst. Des. Eng.* **2019**, *4*, 263–279, DOI: `10.1039/c8me00096d`.

(138) Jones, S. D.; Schauser, N. S.; Fredrickson, G. H.; Segalman, R. A. The Role of Polymer-Ion Interaction Strength on the Viscoelasticity and Conductivity of Solvent-Free Polymer Electrolytes. *Macromolecules* **2020**, *53*, 10574–10581, DOI: `10.1021/acs.macromol.0c02233`.

(139) Kloxin, C. J.; Scott, T. F.; Adzima, B. J.; Bowman, C. N. Covalent Adaptable Networks (CANS): A Unique Paradigm in Cross-Linked Polymers. *Macromolecules* **2010**, *43*, 2643–2653, DOI: `10.1021/ma902596s`.

(140) Kloxin, C. J.; Bowman, C. N. Covalent Adaptable Networks: Smart, Reconfigurable and Responsive Network Systems. *Chem. Soc. Rev.* **2013**, *42*, 7161–7173, DOI: `10.1039/c3cs60046g`.

(141) Winne, J. M.; Leibler, L.; Du Prez, F. E. Dynamic Covalent Chemistry in Polymer Networks: a Mechanistic Perspective. *Polym. Chem.* **2019**, *10*, 6091–6108, DOI: `10.1039/c9py01260e`.

(142) Scheutz, G. M.; Lessard, J. J.; Sims, M. B.; Sumerlin, B. S. Adaptable Crosslinks in Polymeric Materials: Resolving the Intersection of Thermoplastics and Thermosets. *J. Am. Chem. Soc.* **2019**, *141*, 16181–16196, DOI: `10.1021/jacs.9b07922`.

(143) Danielsen, S. P. O. Chemical Compatibilization, Macro-, and Microphase Separation of Hetero-Associative Polymers. *ChemRxiv* **2023**,